Laboratory Investigation (2010) 90, 476–495

Selective intrarenal human A_1 adenosine receptor overexpression reduces acute liver and kidney injury after hepatic ischemia reperfusion in mice

Sang Won Park[1], Sean WC Chen[1], Mihwa Kim[1], Vivette D D'Agati[2] and H Thomas Lee[1]

Acute kidney injury (AKI) is frequent after liver ischemia reperfusion (IR) can potentiate liver injury and is often complicated by subsequent multiorgan dysfunction syndrome. AKI because of liver IR is characterized by early renal endothelial cell apoptosis and impaired vascular integrity with subsequent neutrophil infiltration, proximal tubule necrosis/inflammation, and filamentous (F) actin disintegration. We tested whether selective renal overexpression of human A_1 adenosine receptors (huA_1AR) protects against both liver and kidney injury sustained after liver IR. Mice were subjected to liver IR or to sham surgery 48 h after unilateral intrarenal injection of lentivirus encoding enhanced green fluorescent protein (EGFP) or EGFP-huA_1AR. Intrarenal lentiviral gene delivery caused a robust transgene expression in the injected kidney without significant expression in the contralateral kidney or in the liver. Mice injected with EGFP-huA_1AR lentivirus were protected against hepatic IR-induced liver and kidney injury with reduced necrosis, inflammation, and apoptosis, and better preserved F-actin and vascular permeability compared with mice injected with EGFP lentivirus. Importantly, we show that removing the EGFP-huA_1AR lentivirus-injected kidney before hepatic ischemia abolished both renal and hepatic protection after liver IR showing that the overexpression of huA_1AR in the injected kidney has a crucial role in protecting the kidney and liver after liver IR. Therefore, our findings show that protecting the kidney reduces liver IR injury and selective overexpression of cytoprotective A_1ARs in the kidney leads to protection of both liver and kidney after hepatic IR.

Laboratory Investigation (2010) **90,** 476–495; doi:10.1038/labinvest.2009.143; published online 11 January 2010

KEYWORDS: acute kidney injury; acute liver failure; apoptosis; inflammation; lentivirus; necrosis

Hepatic ischemia and reperfusion (IR) is a frequent cause of acute liver failure during the perioperative period. Patients suffer from hepatic IR in many clinical conditions including liver transplantation, major hepatic resection or prolonged portal vein occlusion.[1,2] The pathophysiology of hepatic IR injury is complex and both hepatic (hepatocytes, Kupffer cells) and extra-hepatic (leukocytes, circulating cytokines) factors have important roles. Hepatic IR frequently leads to remote organ injury including kidney, lung, and heart.[3,4] In particular, acute kidney injury (AKI) or hepatorenal syndrome occurs frequently in patients with acute liver failure (40–85% incidence) and the development of AKI after liver injury greatly increases mortality and morbidity during the perioperative period by potentiating extrarenal organ injury including liver.[5,6] Therefore, injury of one organ (liver or kidney) can cause and potentiate injuries in both organs. We recently developed a murine model of liver IR-induced AKI characterized by early renal endothelial cell apoptosis, proximal tubule inflammation (because of cytokine and neutrophil infiltration), and necrosis.[7] Liver IR-induced AKI also produced severe impairment in vascular permeability together with filamentous (F)-actin degradation of kidney.[7] Therefore, AKI developed because of liver IR seems to be a disease of early renal endothelial cell apoptosis and dysfunction with subsequent F-actin degradation and proximal tubular necrosis/inflammation.

Our laboratory previously showed that exogenous and endogenous A_1 adenosine receptor (A_1AR) activation protected against renal IR injury in mice[8,9] as well as in rats[10,11] with reduced renal tubular necrosis, apoptosis, and

[1]Department of Anesthesiology, College of Physicians and Surgeons of Columbia University, New York, NY, USA and [2]Department of Pathology, College of Physicians and Surgeons of Columbia University, New York, NY, USA
Correspondence: Dr HT Lee, MD, PhD, Department of Anesthesiology, Anesthesiology Research Laboratories, Columbia University, P&S Box 46 (PH-5), 630 West 168th Street, New York, NY 10032-3784, USA.
E-mail: tl128@columbia.edu

Received 3 August 2009; revised 4 November 2009; accepted 19 November 2009

inflammation. Moreover, endogenous A_1ARs have an important role in protecting the liver against IR injury in mice.[12] Therefore, endogenous and exogenous activation of A_1ARs protect against renal as well as hepatic IR injury. We also showed that injection of lentivirus encoding for human A_1ARs (huA_1AR) resulted in a selective expression in the injected kidney and this selective renal expression of A_1ARs attenuated renal IR injury in mice lacking A_1ARs.[13] Therefore, we tested the following hypothesis in this study: overexpression of huA_1ARs in the kidney would protect against AKI after hepatic IR. We questioned whether (1) selective unilateral overexpression of renal A_1ARs in mice through viral gene delivery would increase the resistance against hepatic IR-induced AKI in mice and (2) protecting the kidney would result in reduced liver injury after severe hepatic IR injury.

We used intrarenal gene delivery with a lentiviral vector that expresses either enhanced green fluorescent protein (EGFP) or EGFP-huA_1AR. We subsequently probed for the expression of transgene in the injected kidney and in the liver. We also subjected mice to liver IR injury 48 h after unilateral renal injection with lentivirus encoding EGFP or EGFP-huA_1AR. Finally, we probed the mechanisms of renal protection with EGFP-huA_1AR overexpression by examining whether renal huA_1AR overexpression in mice leads to HSP27 upregulation in the injected kidney. We demonstrate that mice renally injected with EGFP-huA_1AR lentivirus showed (1) significant renal protection after hepatic IR injury with reduced necrosis, inflammation, and renal endothelial cell apoptosis when compared with mice injected with EGFP lentivirus; (2) markedly improved liver function and reduced liver necrosis, apoptosis, and inflammation after liver IR; and (3) upregulation of HSP27 and increased colocalization with huA_1ARs in kidneys injected with EGFP-huA_1AR lentivirus. Therefore, selective unilateral overexpression of A_1ARs in mice through lentiviral delivery protected against both acute liver failure and AKI after liver IR *in vivo*.

METHODS

Detailed methods describing surgery and anesthesia protocols, immunohistochemistry, and RNA isolation are available as Supplementary information.

Intrarenal Lentivirus Delivery *In Vivo*

Lentivirus encoding EGFP or EGFP-huA_1AR was generated as described previously[14,15] (Supplementary information). *In vivo* virus transduction to express huA_1ARs in kidneys of mice was performed as described by Nakamura *et al*[16] with slight modifications as described previously[13] (Supplementary information).

Determination of Transgene Expression with Intrarenal Lentivirus Injection

We used three techniques to detect the expression of EGFP or EGFP-huA_1AR in kidney and liver after intrarenal injection of lentivirus. The following are the three techniques: (1) direct visualization of EGFP in frozen sections, (2) immunohistochemistry for huA_1ARs, and (3) RT–PCR for the EGFP-A_1AR transgene in liver and kidney tissues. Forty-eight hours after lentivirus injection, kidneys and livers were removed, embedded in Tissue-Tek oxytetracycline compound (Fisher Scientific, Suwanee, GA, USA) in dry ice and were cut into 5 μm sections. EGFP expression was directly visualized with a fluorescence microscope (Olympus IX81, Tokyo, Japan), and the images were captured and stored using SlideBook 4.2 software (Intelligent Imaging Innovations, Denver, CO, USA) on a personal computer. Immunohistochemistry for huA_1ARs was performed as described below. Finally, total RNA was extracted from renal cortices or liver and we performed reverse transcription-PCR assays for EGFP-huA_1AR, EGFP and mouse GAPDH as described previously[14,17,18] (Table 1). The EGFP-huA_1AR primer was designed with a sense primer that would anneal in the extreme 5′ end of the A_1AR portion of the construct, whereas the anti-sense primer anneals to the extreme 3′ end of the EGFP portion.

We previously showed that activation and overexpression of A_1ARs led to upregulation of HSP27 expression.[13,14] Therefore, we also determined whether overexpression of huA_1ARs through lentiviral gene delivery resulted in upregulation of mouse HSP27 mRNA expression in the injected kidney with RT–PCR as described previously.[14] We also determined whether the contralateral kidney or liver HSP27 mRNA expression changes after unilateral renal injection of EGFP-huA_1AR lentivirus.

Murine Model of Hepatic IR

All protocols were approved by the Institutional Animal Care and Use Committee of Columbia University. Two days after intrarenal injection of lentivirus encoding EGFP or EGFP-huA_1AR into the left kidney, male C57BL/6 mice (20–25 g; Harlan, Indianapolis, IN, USA) were subjected to liver IR injury as described previously[7] (Supplementary information). Sham-operated mice were subjected to laparotomy and identical liver manipulations without the vascular occlusion. In some mice, we removed the EGFP or EGFP-huA_1AR lentivirus-injected left kidney before liver ischemia to determine whether the EGFP-huA_1AR overexpressing kidneys are directly responsible for reducing liver and kidney injury after liver IRI.

Twenty-four hours after reperfusion, the liver tissue subjected to IR and kidneys were collected to measure necrosis, neutrophil infiltration (with immunohistochemistry), vascular permeability, apoptosis (with terminal deoxynucleotidyl transferase-mediated dUTP nick end-labeling staining, DNA laddering, and caspase 3 protein cleavage), and F-actin integrity. In some mice, liver and kidneys were collected 5 h after reperfusion to detect inflammatory changes by RT–PCR for proinflammatory cytokine mRNAs. We also collected plasma for the measurement of alanine

Table 1 RT–PCR primers used in this study

Genes	Species	Amplicon size (bp)	Primer sequences (sense/antisense)	Annealing °C/no. of cycles
GAPDH	Mouse	450	5′-ACCACAGTCCATGCCATCAC-3′	65/15
			5′-CACCACCCTGTTGCTGTAGCC-3′	
A_1AR	Mouse	340	5′-CATTGGGCCACAGACCTACT-3′	60/22
	Human		5′-GAAGTAGACCATGTACTCCA-3′	
EGFP-huA_1AR	Viral construct for human A_1AR	540	5′-TGCCTTTGCACATCCTCAAC-3′	64/40
			5′-AAGTCGTGCTGCTTCATGTG-3′	
TNF-α	Mouse	290	5′-TACTGAACTTCGGGGTGATTGGTCC-3′	65/24
			5′-CAGCCTTGTCCCTTGAAGAGAACC-3′	
ICAM-1	Mouse	409	5′-TGTTTCCTGCCTCTGAAGC-3′	60/21
			5′-CTTCGTTTGTGATCCTCCG-3′	
KC	Mouse	203	5′-CAATGAGCTGCGCTGTCAGTG-3′	60/26
			5′-CTTGGGGACACCTTTTAGCATC-3′	
MCP-1	Mouse	312	5′-ACCTGCTGCTACTCATTCAC-3′	60/22
			5′-TTGAGGTGGTTGTGGAAAAG-3′	
MIP-2	Mouse	282	5′-CCAAGGGTTGACTTCAAGAAC-3′	60/25
			5′-AGCGAGGCACATCAGGTACG-3′	
HSP27	Mouse	373	5′-CCTAAGGTCTGGCATGGTA-3′	66/25
			5′-AGGAAGCTCGTTGTTGAAGC-3′	

A_1AR, A_1 adenosine receptor; GAPDH, glyceraldehyde 3-phosphate dehydrogenase; HSP27, heat shock protein 27; ICAM-1, intercellular adhesion molecule-1; KC, keratinocyte-derived chemokine; MCP-1, monocyte chemoattractant protein 1; MIP-2, macrophage inflammatory protein 2; TNF-α, tumor necrosis factor alpha.

aminotransferase (ALT) and creatinine at 5 and 24 h after reperfusion.

Plasma ALT Activity and Creatinine Level

The plasma ALT activities were measured using the Infinity™ ALT assay kit according to the manufacturer's instructions (Thermo Fisher Scientific, Waltham, MA, USA). Plasma creatinine was measured by an enzymatic creatinine reagent kit according to the manufacturer's instructions (Thermo Fisher Scientific). This method of creatinine measurement largely eliminates the interferences from mouse plasma chromagens well known to the Jaffe method.[19]

Histological Analysis of Hepatic and Renal Injury

For histological preparations, liver or kidney tissues were fixed in 10% formalin solution overnight. After automated dehydration through a graded alcohol series, transverse liver slices were embedded in paraffin, sectioned at 4 μm, and stained with hematoxylin and eosin (H&E). Liver H&E sections were graded for IR injury by a pathologist (VDD) who was blinded to the samples using the system devised by Suzuki *et al*.[20] In this classification, three liver injury indices are graded: sinusoidal congestion (0–4), hepatocyte necrosis (0–4), and ballooning degeneration (0–4) are graded for a total score of 0–12. No necrosis, congestion, or centrilobular ballooning is given a score of 0 whereas severe congestion/ballooning and >60% lobular necrosis are each given a value of 4. Renal H&E sections were evaluated for the severity (score: 0–3) of renal cortical vacuolization, peritubular/proximal tubule leukocyte infiltration, percentage of proximal tubule simplification and proximal tubule hypereosinophilia by an experienced pathologist (VDD) who was blinded to the treatment each animal had received.

Enzyme Linked Immunosorbent Assay For Plasma, Liver and Kidney TNF-α MCP-1 and ICAM-1

After 5 and 24 h of liver reperfusion, the plasma, liver, and lentivirus-injected kidney tissue TNF-α, MCP-1, and ICAM-1 levels were measured with mouse specific ELISA kits according to the manufacturer's instructions (eBiosciences, San Diego, CA, USA). We also measured plasma cytokine levels in mice subjected to nephrectomy of the lentivirus-injected kidney and hepatic ischemia and 24 h reperfusion. Liver and kidney tissues were homogenized in ice-cold RIPA buffer (150 mM NaCl, 50 mM Tris-HCl, 1 mM EDTA, and 1% Triton-X (pH 7.4)) and samples processed for mouse specific ELISA kits.

Assessment of Liver and Kidney Inflammation

Liver and kidney inflammation after hepatic ischemia was determined by the detection of neutrophil infiltration by immunohistochemistry 24 h after hepatic IR as described

previously[7] and by measuring mRNA encoding markers of inflammation, including keratinocyte-derived cytokine (KC), intercellular adhesion molecule-1 (ICAM-1), monocyte chemoattractive protein-1 (MCP-1), macrophage inflammatory protein-2 (MIP-2), and TNF-α 5 h after liver IR as described[7] (Supplementary information).

Kidney and Liver Tissue Immunoblotting Analyses for HSP27 and β-Actin

Forty-eight hours after lentivirus injection, liver tissues or mouse kidney tissues (lentivirus-injected left kidney and contralateral right kidney) were dissected on ice and immediately placed in ice-cold RIPA buffer (150 mM NaCl, 50 mM Tris-HCl, 1 mM EDTA, and 1% Triton-X (pH 7.4)) and homogenized for 10 s on ice. The samples were centrifuged for 30 min at 50 000 *g*. The supernatant was collected and used for immunoblotting of mouse HSP27 (primary antibody from Millipore, Billerica, MA, USA) and β-actin (primary antibody from Sigma, St Louis, MO, USA, as protein loading control) as described previously.[7,14]

Vascular Permeability of Liver and Kidney Tissues

Changes in liver and kidney vascular permeability were assessed by quantitating extravasation of Evans blue dye (EBD) into the tissue as described by Awad *et al*[21] with some modifications as described[22] (Supplementary information).

Detection of Liver and Kidney Apoptosis

We used three independent assays to assess the degree of liver and kidney apoptosis after IR: *in situ* Terminal Deoxynucleotidyl Transferase Biotin-dUTP Nick End-Labeling (TUNEL) assay, detection of DNA laddering, and immunoblotting for fragmented caspase 3 as describe previously[7,14] (Supplementary information). For DNA laddering, liver and kidney tissues were removed 24 h after liver IR, apoptotic DNA fragments were extracted according to the methods of Herrmann *et al*.[23] This method of DNA extraction selectively isolates apoptotic, fragmented DNA and leaves behind the intact chromatin. We also performed β-actin immunoblotting to confirm equal protein loading in our caspase 3 immunoblotting experiments.

F-Actin Staining of Liver and Kidney Sections

As breakdown of F-actin occurs early after IR, we visualized the F-actin cytoskeleton by staining with phalloidin as an early index of liver as well as renal injury[24] as described previously[22] (Supplementary information).

Immunohistochemistry for HSP27 and huA_1AR

Forty-eight hours after intrarenal lentivirus injection, immunohistochemistry for murine HSP27 and huA_1AR were performed as described previously[13] (Supplementary information).

Protein Determination

Protein contents were determined with a bicinchoninic acid protein assay kit (Pierce Chemical, Rockford, IL, USA), using bovine serum albumin as a standard.

Statistical Analysis

The data were analyzed with *t*-test when means between two groups were compared or with one-way (eg, plasma creatinine or ALT) ANOVA and Tukey's *post hoc* multiple comparison test to compare mean values across multiple treatment groups. In all cases, $P<0.05$ was taken to indicate significance. All data are expressed as mean ± s.e.m.

Reagents

Unless otherwise specified, all chemicals were obtained from Sigma.

RESULTS

Selective *In Vivo* Renal Expression of EGFP or EGFP-huA_1AR after Intrarenal Lentiviral Gene Delivery in Mice

None of the mice died or showed signs of AKI after lentiviral injection to their kidneys. We first determined in this study that selective intrarenal injection of lentivirus produced robust expression of the transgene in the injected kidney without significant expression in the right kidney or in the liver. Figure 1a shows that intrarenal delivery of lentivirus encoding EGFP or EGFP-huA_1AR resulted in a robust and selective expression of transgene in the renal cortical areas (cortex and corticomedullary junction) of the injected kidneys. The transgene expression was very low in the medulla (concentration of collecting ducts and thin limbs of Henle) of injected kidneys. Furthermore, predominant membrane/cytosolic (green) localization but not nuclear (dark) expression of EGFP-huA_1AR was observed after lentivirus injection. In the liver (Figure 1b), the transgene expression was undetectable (similar to baseline green auto-fluorescence) 48 h after lentiviral injection into the left kidney. Moreover, we failed to observe green fluorescence in the contralateral kidney (Figure 1a), heart or lungs (not shown) of mice renally injected with lentiviruses encoding these constructs.

Figure 1c shows the expression of EGFP-huA_1AR mRNA with primers designed to selectively amplify this transgene (detected with RT–PCR, 40 cycle amplification) in the renal cortices of mice renally injected with the EGFP-huA_1AR lentivirus but not in the renal cortices of mice injected with the EGFP lentivirus. Contralateral kidneys or livers of EGFP-huA_1AR lentivirus-injected mice did not show any expression of EGFP-huA_1AR transgene detected with 40 cycles of RT–PCR (data not shown). Mice renally injected with the EGFP-huA_1AR or EGFP lentivirus show EGFP mRNA in the renal cortices (Figure 1c).

We also confirmed the expression of huA_1ARs in EGFP-huA_1AR renally injected mice by performing immunohistochemistry with an antibody specific for huA_1ARs.

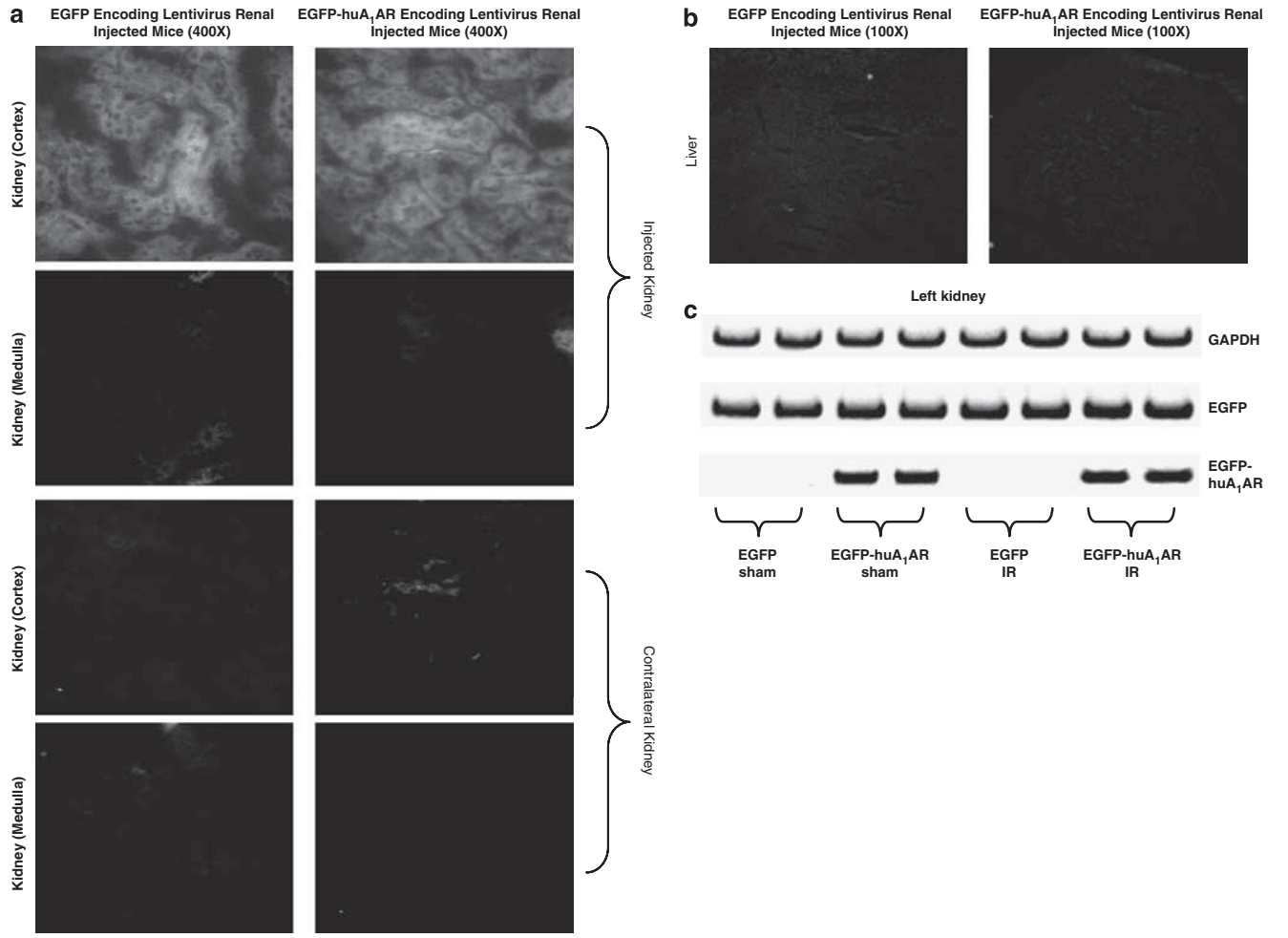

Figure 1 (**a**) Representative kidney fluorescent photomicrographs of four experiments from mice (magnification of $\times 400$) showing predominant localization of EGFP expression in the cortex and corticomedullary junction with relative sparing of the medullary areas. Predominant membrane/cytosolic (green) localization but not nuclear (dark) expression of EGFP-huA$_1$AR was observed after lentivirus injection. (**b**) Representative liver fluorescent photomicrographs of four experiments from mice (magnification of $\times 400$) showing lack of EGFP visualization. C57BL/6 mice kidneys were renally injected with EGFP encoding lentivirus or EGFP-huA$_1$AR encoding lentivirus and 48 h later, their kidneys or liver were embedded in oxytetracycline compound. (**c**) Representative gel images of RT–PCR results from six experiments for GAPDH, EGFP, and EGFP-huA$_1$AR from mice renal cortices. C57BL/6 mouse kidneys were injected with EGFP encoding lentivirus or EGFP-huA$_1$AR encoding lentivirus 48 h before RT–PCR. The EGFP-huA$_1$AR primer was designed with a sense primer that would anneal in the extreme 5′ end of the A$_1$AR portion of the construct, whereas the antisense primer anneals to the extreme 3′ end of the EGFP portion.

Figure 2 shows that the mice injected with EGFP-huA$_1$AR lentivirus show a robust expression of huA$_1$ARs (red) whereas the mice injected with EGFP lentivirus failed to show any expression. Furthermore, with 0.25 μm *Z*-sections, we were able to show that huA$_1$ARs (red) and EGFP (green) colocalize together (yellow, Figure 2f).

Unilateral Renal Injection of EGFP-huA$_1$AR Lentivirus Protects against Hepatic and Renal Injury after Liver IR

The average plasma level of ALT in the sham-operated mice renally injected with lentivirus encoding EGFP and EGFP-huA$_1$AR was 65 ± 12 U/L ($N=6$) and 72 ± 8 U/L ($N=6$), respectively. The average plasma level of Cr in the sham-operated mice renally injected with lentivirus encoding EGFP and EGFP-huA$_1$AR was 0.54 ± 0.04 mg/dl ($N=6$) and 0.52 ± 0.07 mg/dl ($N=6$), respectively. In mice renally injected with EGFP lentivirus, the plasma level of ALT significantly increased at 5 h (ALT $= 19673 \pm 1558$ U/L, $N=10$, $P<0.0001$ *vs* Sham) and 24 h (ALT $= 15432 \pm 753$ U/L, $N=10$, $P<0.0001$ *vs* Sham) after liver IR (Figure 3). Moreover, mice renally injected with EGFP lentivirus developed AKI 24 h after liver IR (Cr $= 1.06 \pm 0.12$ mg/dl, $N=13$, $P<0.01$ *vs* Sham, Figure 3). The increases in ALT were significantly suppressed in mice renally injected (48 h before liver IR) with EGFP-huA$_1$AR lentivirus at 5 h (ALT $= 12794 \pm 1017$ U/L, $N=8$, $P<0.01$) and 24 h (ALT $= 6663 \pm 755$ U/L, $N=8$, $P<0.001$) after liver IR (Figure 3). The increases in Cr were also significantly sup-

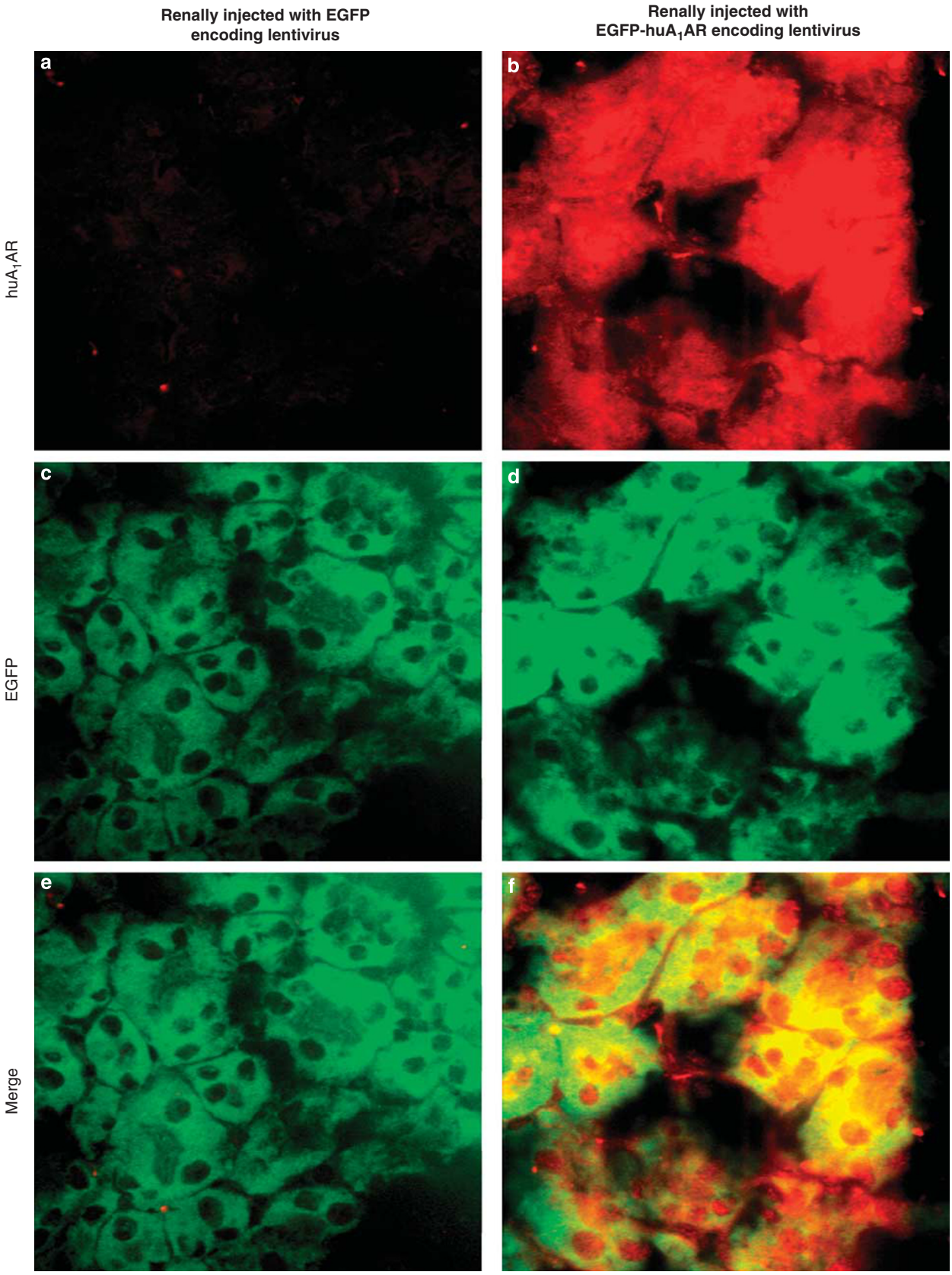

Figure 2 Representative of four immunohistochemistry fluorescence photomicrographs for huA$_1$ARs (red, **a**, **b**) and EGFP expression (green, **c**, **d**) in C57BL/6 mice that are renally injected with either EGFP (**a**, **c**, **e**) or EGFP-huA$_1$AR lentivirus (**b**, **d**, **f**) before 48 h. With 0.25 μm thick *Z*-sections, we were able to show that huA$_1$ARs (red) and EGFP (green) colocalize together (yellow, **e**, **f**).

pressed at 24 h after liver IR by injecting left kidney with EGFP-huA$_1$AR lentivirus (Cr = 0.44 ± 0.07 mg/dl, $N = 8$, $P < 0.01$; Figure 3).

Unilateral Renal Injection of EGFP-huA$_1$AR Lentivirus Reduces TNF-α, MCP-1, and ICAM-1 Levels in Plasma, Liver, and Lentivirus-Injected Kidney after Liver IR

In sham-operated animals, plasma and tissue (liver and kidney) TNF-α, MCP-1, and ICAM-1 levels were very low or undetectable (Table 2). In contrast, plasma and liver TNF-α MCP-1 and ICAM-1 levels increased 5 and 24 h after liver IR in EGFP lentivirus-injected mice (Table 2). However, these increases at both 5 and 24 h were significantly attenuated in mice with unilateral renal injection of EGFP-huA$_1$AR lentivirus and subjected to hepatic IR. Moreover, renal TNF-α increased 24 h after liver IR in EGFP lentivirus-injected mice, which was reduced in mice with unilateral renal injection of EGFP-huA$_1$AR lentivirus and subjected to hepatic IR (Table 2). We also measured the plasma cytokine levels in mice after removing the lentivirus-injected kidney and subjected to liver IR (Table 2). We show that mice subjected to unilateral nephrectomy and hepatic IR show increased plasma TNF-α, MCP-1, and ICAM-1 protein compared with mice with two intact kidneys (Table 2). Furthermore, elimination of EGFP-huA$_1$AR lentivirus-injected kidney abolishes the reductions in proinflammatory cytokines (TNF-α and MCP-1) and ICAM-1 in mice after liver IR (Table 2).

Removing EGFP-huA$_1$AR Lentivirus-Injected Kidney before Hepatic Ischemia Abolishes Both Renal and Hepatic Protection after Liver IR

We tested whether removing the lentivurus injected kidney would impact renal and hepatic injury after liver IR. Unilateral nephrectomy of the EGFP lentivirus-injected kidney before hepatic ischemia did not significantly change the hepatic (ALT = 15049 ± 1180 U/L, $N = 4$) and renal injury (Cr = 1.32 ± 0.15 mg/dl, $N = 4$) compared with the EGFP lentivirus-injected mice with two intact kidneys (Figure 3) 24 h after reperfusion. However, unilateral nephrectomy of the EGFP-huA$_1$AR lentivirus-injected kidney before hepatic ischemia completely abolished the hepatic (ALT = 13013 ± 792 U/L, $N = 4$) and renal (Cr = 1.12 ± 0.11 mg/dl, $N = 4$) protective effects of renal huA$_1$AR overexpression (Figure 3) showing that the overexpression of huA$_1$AR in the injected kidney has a crucial role in protecting the kidney and liver after liver IR. The ALT and Cr values in mice after EGFP or EGFP-huA$_1$AR lentivirus injection and uninephrectomy alone were not different.

Unilateral Renal Injection of EGFP-huA$_1$AR Lentivirus Reduces Hepatic Necrosis after Liver IR

Representative histological slides (magnification, × 200 and × 600) from liver tissues from mice renally injected with EGFP lentivirus or EGFP-huA$_1$AR lentivirus and

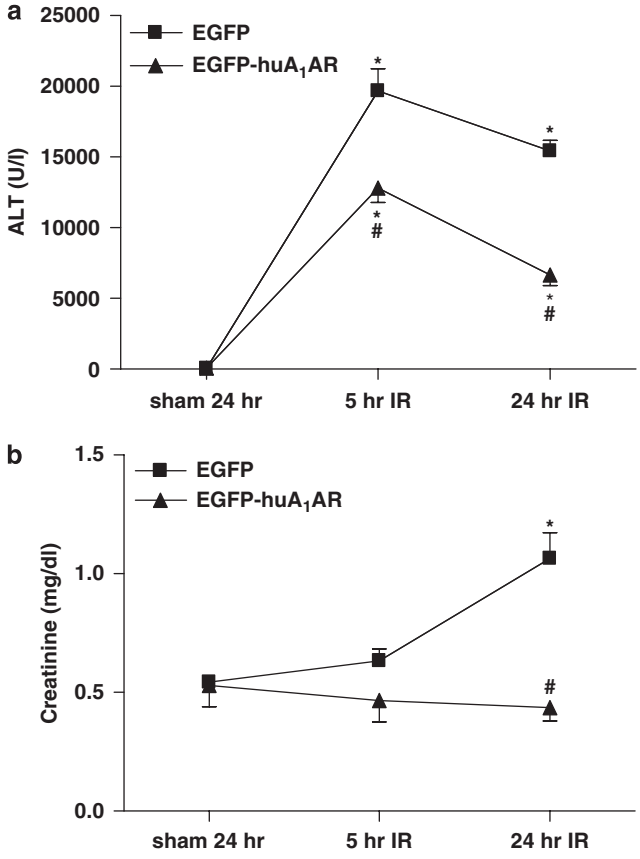

Figure 3 Plasma ALT (**a**, U/L) and creatinine (**b**, mg/dL) levels in C57BL/6 mice injected with EGFP encoding lentivirus or EGFP-huA$_1$AR encoding lentivirus and subjected to sham-operation (Sham) or liver ischemia–reperfusion (IR) injury. Mice were subjected to sham-surgery ($N = 6$ each) or liver IR 48 h after renal injection with EGFP ($N = 10$) or EGFP-huA$_1$AR ($N = 8$) encoding lentivirus and plasma ALT and creatinine was measured 5 or 24 h after reperfusion. $^*P < 0.05$ *vs* appropriate sham-operated mice. $^\#P < 0.05$ *vs* EGFP injected mice subjected to liver IR. Data presented as mean ± s.e.m.

subjected to 60 min liver ischemia and 24 h reperfusion are shown in Figure 4. Sixty minutes of partial hepatic IR produced large necrotic areas and vacuolization in the liver after reperfusion (Figure 4). Correlating with significantly improved function, reduced hepatic necrosis, and vacuolization were observed in mice renally injected with EGFP-huA$_1$AR and subjected to hepatic IR (Figure 4). We failed to detect necrosis in liver sections from sham-operated mice renally injected with EGFP or EGFP-huA$_1$AR lentivirus (not shown). Livers were also analyzed for the degree of hepatocellular damage using Suzuki's criteria.[25] The ischemic lobes in the control group showed severe hepatocyte necrosis and sinusoidal congestion (Suzuki score = 8.6 ± 0.5, $N = 5$). Mice injected with EGFP-huA$_1$AR revealed significantly less necrosis/sinusoidal congestion and better preservation of lobular architecture (Suzuki score = 6.8 ± 0.5, $N = 5$, $P < 0.05$).

Table 2 ELISA results

	Groups	TNF-α (pg/ml)	MCP-1 (pg/ml)	ICAM-1 (pg/ml)
Plasma	EGFP sham	25.6 ± 13.4	0.0 ± 0.0	233.5 ± 147.7
	EGFP-huA$_1$AR sham	47.7 ± 24.0	0.0 ± 0.0	46.6 ± 29.5
	EGFP IR 5 h	207.6 ± 38.0*	196.4 ± 46.4*	2718.7 ± 300.2*
	EGFP-huA$_1$AR IR 5 h	47.6 ± 18.3$^{\#}$	55.8 ± 18.5$^{*,\#}$	1765.7 ± 389.8$^{*,\#}$
	EGFP IR 24 h	674.3 ± 26.8*	361.8 ± 74.0*	3783.9 ± 334.8*
	EGFP-huA$_1$AR IR 24 h	331.2 ± 113.9$^{*,\#}$	113.7 ± 35.8$^{*,\#}$	1821.7 ± 237.9$^{*,\#}$
	1 Nx EGFP IR 24 h	1441.3 ± 292.9$^{*,\#}$	867.4 ± 167.4$^{*,\#}$	6119.9 ± 208.1$^{*,\#}$
	1 Nx EGFP-huA$_1$AR IR 24 h	1824.6 ± 163.6$^{*,\#}$	807.3 ± 246.2$^{*,\#}$	5708.8 ± 208.1$^{*,\#}$
		(pg/mg protein)	(pg/mg protein)	(pg/mg protein)
Liver	EGFP sham	0.0 ± 0.0	0.0 ± 0.0	4.5 ± 2.8
	EGFP-huA$_1$AR sham	0.0 ± 0.0	0.0 ± 0.0	7.1 ± 4.5
	EGFP IR 5 h	47.0 ± 11.6*	43.8 ± 7.7*	67.4 ± 15.0*
	EGFP-huA$_1$AR IR 5 h	13.3 ± 2.6$^{*,\#}$	25.0 ± 1.9$^{*,\#}$	58.0 ± 13.7*
	EGFP IR 24 h	51.1 ± 6.1*	80.8 ± 8.8*	168.9 ± 34.8*
	EGFP-huA$_1$AR IR 24 h	30.0 ± 5.8$^{*,\#}$	48.9 ± 3.6$^{*,\#}$	83.3 ± 10.0$^{*,\#}$
Kidney	EGFP sham	1.4 ± 0.9	0.0 ± 0.0	32.3 ± 11.9
	EGFP-huA$_1$AR sham	0.0 ± 0.0	0.0 ± 0.0	27.9 ± 17.7
	EGFP IR 5 h	2.6 ± 1.7	57.1 ± 4.5*	164.3 ± 18.5*
	EGFP-huA$_1$AR IR 5 h	1.3 ± 0.8	16.2 ± 2.2$^{*,\#}$	39.2 ± 3.6$^{*,\#}$
	EGFP IR 24 h	20.3 ± 2.2*	89.7 ± 9.0*	202.5 ± 30.4*
	EGFP-huA$_1$AR IR 24 h	14.9 ± 0.0$^{*,\#}$	38.8 ± 3.9$^{*,\#}$	69.7 ± 10.4$^{*,\#}$

ELISA results for TNF-α, MCP-1, and ICAM-1 analyzed from plasma (A, pg/ml, $N = 4$), lentivirus-injected kidney (B, pg/mg protein, $N = 4$) and liver (C, pg/mg protein, $N = 4$) in C57BL/6 mice subjected to sham-operation (Sham) or liver ischemia–reperfusion (IR) injury.

Mice were subjected to sham surgery ($N = 4$ each) or liver IR 48 h after renal injection with EGFP ($N = 5$) or EGFP-huA$_1$AR ($N = 5$) encoding lentivirus. TNF-α, MCP-1, and ICAM-1 levels were analyzed 5 or 24 h after reperfusion.

1 Nx, uninephrectomy of the lentivirus injected kidney before liver IR.

*$P < 0.05$ *vs* appropriate sham-operated mice.

$^{\#}P < 0.05$ *vs* respective 5 or 24 h EGFP-injected mice subjected to liver IR.

Data presented as mean ± s.e.m.

Unilateral Renal Injection of EGFP-huA$_1$AR Lentivirus Reduces Renal Cortical Vacuolization, Proximal Tubular Simplification, and Proximal Tubular Hypereosinophilia after Liver IR

Representative H&E slides from kidneys from mice renally injected with EGFP and EGFP-huA$_1$AR lentivirus and subjected to 60 min ischemia and 24 h reperfusion are shown in Figure 5a (injected left kidney, × 400). When we examined the kidneys from the mice injected with EGFP encoding lentivirus and subjected to liver IR, we observed multifocal acute tubular injury including S3 segment proximal tubule necrosis, cortical tubular simplification, cytoplasmic vacuolization, and dilated lumina in the injected (left; Figure 5A) kidneys. Correlating with significantly improved renal function, mice renally injected with EGFP-huA$_1$AR lentivirus showed less renal tubular hypereosinophilia, peritubular leukocyte margination, and cortical vacuolization in the injected left kidney (Figure 5a). The summary of renal injury scores for percentage of renal tubular hypereosinophilia, percentage of peritubular leukocyte margination, and percentage cortical vacuolization are shown in Figure 5b.

Unilateral Renal Injection of EGFP-huA$_1$AR Lentivirus Reduces Hepatic and Renal Neutrophil Infiltration 24 h after Liver IR

Figure 6 shows representative images of neutrophil immunohistochemitry of liver (A, magnification × 100) and kidney (B: injected kidney, magnification × 400) from mice subjected to sham-operation or to 60 min of liver ischemia and 24 h reperfusion. Stained neutrophils seem dark brown. In sham-operated mice, we were unable to detect any neutrophils in liver or kidney. Sixty minutes of hepatic ischemia and 24 h reperfusion resulted in a heavy recruitment of

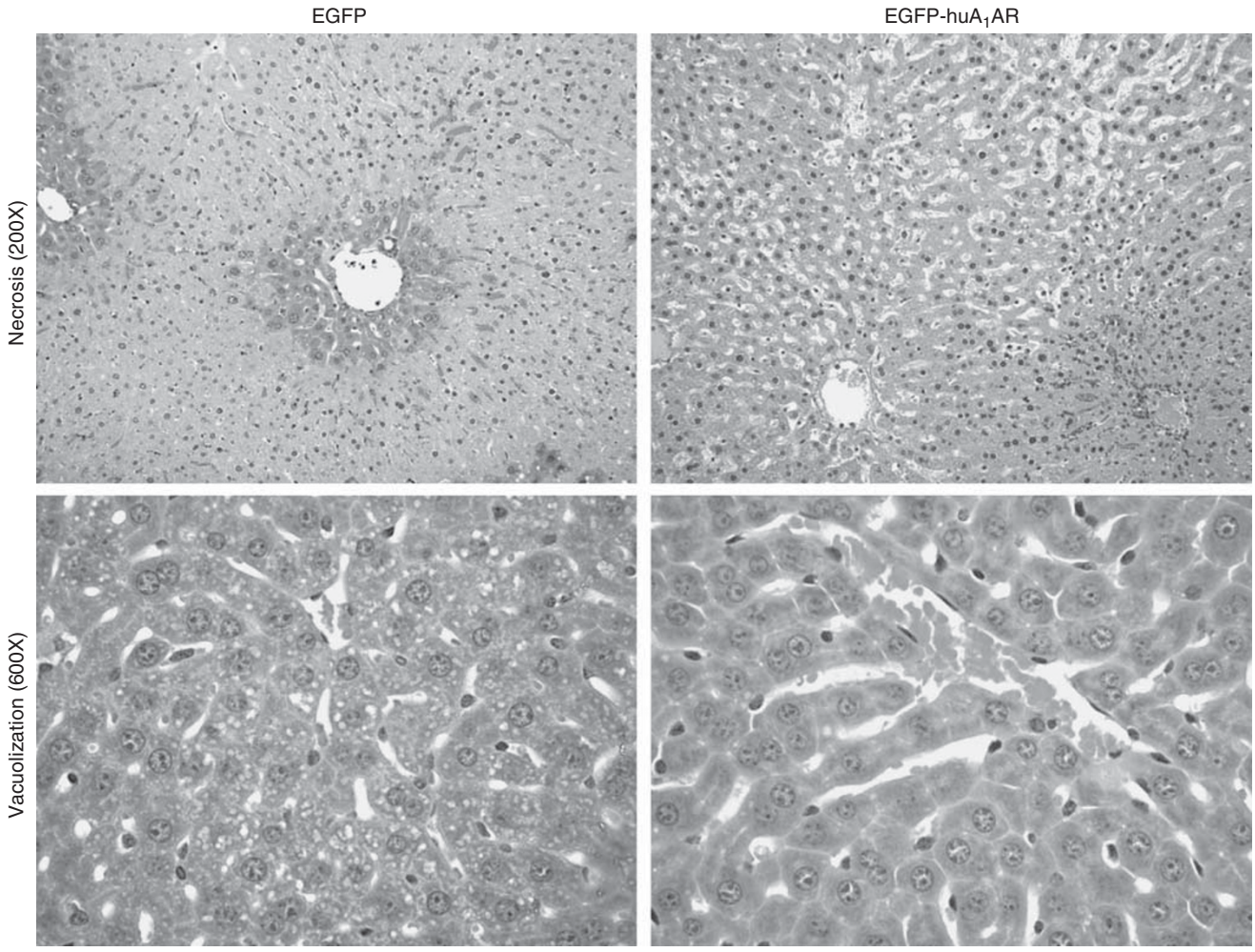

Figure 4 Representative photomicrographs of hematoxylin and eosin (H&E) staining of the liver sections showing necrosis (× 200) and vacuolization (× 600) from C57BL/6 mice subjected to liver IR 48 h after intrarenal injection with EGFP encoding lentivirus or EGFP-huA$_1$AR encoding lentivirus. Photographs are representative of six independent experiments.

neutrophils into liver from mice renally injected with EGFP lentivirus (44 ± 9 neutrophils/field, $\times 100$ magnification, $N = 6$). Mice renally injected with EGFP-huA$_1$AR lentivirus showed reduced number of neutrophils infiltrating the liver (13 ± 3 neutrophils/field, $\times 100$ magnification, $N = 6$, $P < 0.01$). Sixty minutes of hepatic ischemia also resulted in recruitment of neutrophils into kidney (Figure 6b; injected kidney, magnification $\times 400$). Neutrophil infiltration 24 h after hepatic ischemia was significantly less in kidneys of mice renally injected with EGFP-huA$_1$AR lentivirus compared with kidneys from mice renally injected with EGFP lentivirus and subjected to liver IR. Twenty-four hours after liver IR, we detected 14 ± 5 neutrophils/field ($\times 200$ magnification, $N = 6$) in kidney from mice renally injected with EGFP lentivirus and subjected to liver IR. The kidneys injected with EGFP-huA$_1$AR lentivirus showed significantly reduced neutrophil infiltration 24 h after liver IR (2 ± 1 neutrophils/field, $\times 200$ magnification, $N = 6$, $P < 0.05$).

Unilateral Renal Injection of EGFP-huA$_1$AR Lentivirus Decreases Hepatic and Renal Vascular Permeability after Liver IR

We measured liver and kidney vascular permeability after liver IR with EBD injection. EBD binds to plasma proteins and its appearance in extravascular tissues reflects an increase in vascular permeability. Liver IR increased the EBD content in the liver for both groups, however, the increase in EBD content was significantly higher for the EGFP injected mice (478 ± 16 μg EBD per g dry liver, $N = 6$) compared with the EGFP-huA$_1$AR lentivirus-injected mice (348 ± 17 μg EBD per g dry liver, $N = 6$, $P < 0.01$). Liver IR also increased the EBD content in kidneys from both groups. However, the increase in EBD content was significantly higher for EGFP lentivirus renally injected kidney (95 ± 6 μg EBD per g dry kidney, $N = 6$) compared with the EGFP-huA$_1$AR lentivirus renally injected kidneys (71 ± 5 μg EBD per g dry kidney, $N = 6$, $P < 0.01$).

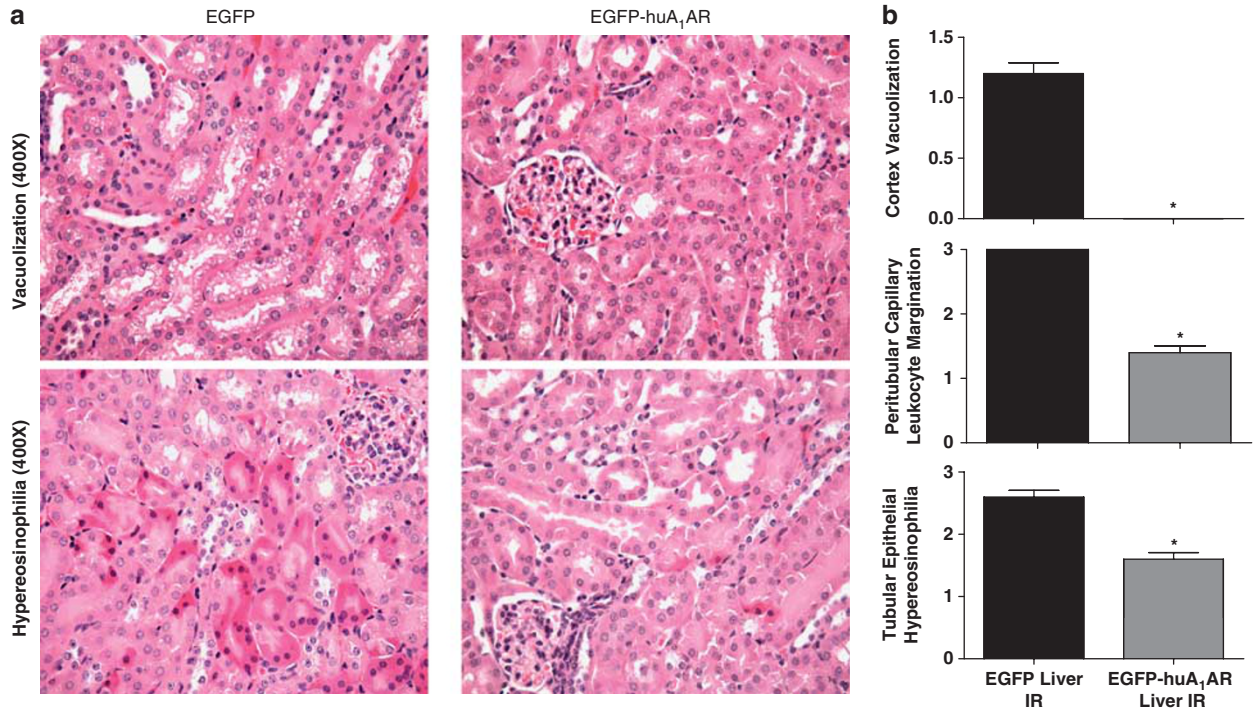

Figure 5 (**a**) Representative photomicrographs of six experiments (hematoxylin and eosin (H&E) staining, magnification × 400) showing vacuolization and proximal tubular hypereosinophillia in kidneys from C57BL/6 mice subjected to liver IR 48 h after intrarenal injection with EGFP lentivirus or EGFP-huA$_1$AR lentivirus. Pictures of the renal cortices of kidneys subjected to renal ischemia–reperfusion (IR) injury before 24 h are shown for the lentivirus-injected left kidneys. (**b**) The summary of renal injury scores for percentage of renal tubular hypereosinophilia, percentage of peritubular leukocyte margination, and percentage of cortical vacuolization for the injected kidneys are shown.

Unilateral Renal Injection of EGFP-huA$_1$AR Lentivirus Reduces TNF-α, ICAM-1, and MCP-1 mRNA in the Liver and in the Injected Kidney after Liver IR

We measured the expression of proinflammatory cytokine mRNAs in liver and kidney 5 h after liver IR with semi-quantitative RT–PCR. Hepatic IR was associated with significantly increased proinflammatory mRNA expression (ICAM-1, TNF-α, KC, MCP-1, and MIP-2) in liver (Figure 7) and kidney (Figure 8) compared with the sham-operated mice. However, mice renally injected with EGFP-huA$_1$AR lentivirus showed significantly reduced TNF-α ICAM-1 and MCP-1 mRNA in the liver (Figure 7a and b) and in the injected (left) kidney (Figure 8a and b) compared with liver and kidneys injected with EGFP lentivirus after liver IR. There were no significant differences in KC or MIP-2 mRNAs.

Unilateral Renal Injection of EGFP-huA$_1$AR Lentivirus Reduces Hepatic and Renal Apoptosis after Liver IR

We used three separate indices to detect apoptosis: TUNEL staining, DNA laddering, and caspase 3 fragmentation in mice renally injected with EGFP or EGFP-huA$_1$AR lentivirus and subjected to 60 min liver ischemia and 24 h of reperfusion. Hepatic IR and 24 h of reperfusion 48 h after EGFP lentivirus injection resulted in significant apoptosis in liver and kidney. The TUNEL staining showed that endothelial cell apoptosis was predominant in kidney. Unilateral renal injection of EGFP-huA$_1$AR lentivirus significantly reduced the apoptosis in liver and in lentivirus-injected kidney with reduced TUNEL staining (Figure 9), DNA laddering (Figure 10), and caspase 3 fragmentation (Figure 11).

Unilateral Renal Injection of EGFP-huA$_1$AR Lentivirus Reduces the Degradation of Hepatic and Renal F-Actin after Liver IR

Liver staining in sham-operated mice after injection with lentivirus encoding EGFP or EGFP-huA$_1$AR shows localization of F-actin at the hepatocyte basolateral membranes and the bile canalicular membranes (Figure 12a). As expected, 60 min of liver ischemia and 24 h of reperfusion resulted in severe disruption of liver parenchymal F-actin compared with the sham-operated mice (Figure 12a; representative of six experiments) in mice renally injected with EGFP encoding lentivirus as the staining of basolateral hepatocyte membranes as well as bile canalicular membranes is strongly decreased and disorganized. However, mice renally injected with EGFP-huA$_1$AR and subjected to liver IR show significantly better preserved F-actin structure after liver IR as staining is quite similar to that of sham-operated mice. Liver IR also resulted in a severe loss of F-actin in renal proximal tubules in 24 h. In Figure 12b, 24 h post-hepatic IR-induced disruptions of F-actin cytoskeleton in renal proximal tubular

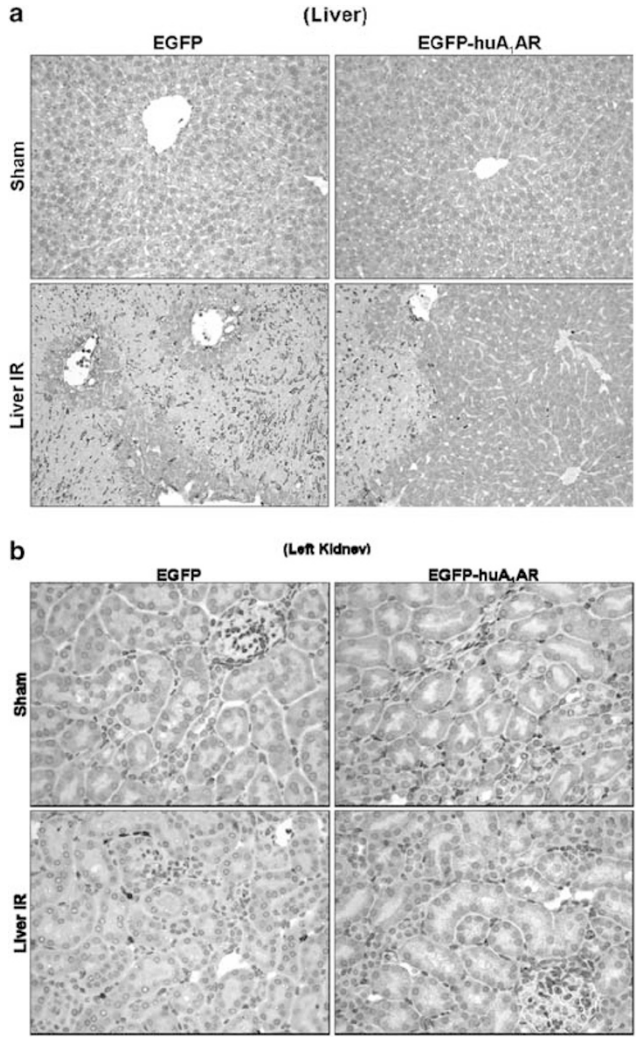

Figure 6 Representative of photomicrographs of immunohistochemistry for neutrophils in liver (**a**, $\times 200$) and lentivirus-injected kidney (**b**, $\times 400$) sections. Stained neutrophils seem dark brown. C57BL/6 mice were subjected to sham-operation (sham) or liver IR 48 h after intrarenal injection with EGFP lentivirus or EGFP-huA$_1$AR lentivirus. The liver and lentivirus-injected kidney sections were obtained 24 h after reperfusion. Photographs are representative of six independent experiments.

epithelial cells are shown. Mice subjected to sham surgery showed intense stain in tubular epithelial cells and in the basal plasma membrane. In contrast, kidneys from mice renally injected with EGFP encoding lentivirus mice subjected to liver IR showed loss of F-actin staining in the tubular epithelial cells. However, mice renally injected with EGFP-huA$_1$AR showed significantly better preserved F-actin structure after liver IR as the staining is quite similar to that of sham-operated mice. Mean flurorescent F-actin intensity showed reduced hepatocyte and renal proximal tubule F-actin degradation in mice renally injected with EGFP-huA$_1$AR after liver IR (Figure 12c and f). We also show that the mice renally injected with EGFP-huA$_1$AR lentivirus show improved preservation of bile canalicular membrane F-actin number as well as fluorescent intensity (Figure 12d and e).

Unilateral Renal Injection of EGFP-huA$_1$AR Lentivirus Leads to Increased HSP27 mRNA and Protein Expression and Colocalization of EGFP-A$_1$AR With HSP27 in the Injected Kidney

As A$_1$AR activation or overexpression results in HSP27 mRNA upregulation,[13,14] we determined whether EGFP-huA$_1$AR lentivirus injection increases HSP27 mRNA as well as protein expression in the injected kidneys by performing RT–PCR and immunoblotting for mouse HSP27. Figure 13 shows that injection of EGFP-huA$_1$AR lentivirus in mice resulted in increased HSP27 mRNA (A) and HSP27 protein (B) expression compared with EGFP lentivirus-injected mice kidneys 48 h after the transgene injection. We also examined the contralateral kidney (nonlentivirus-injected kidney) or liver and demonstrate that these organs failed to show enhanced HSP27 expression (Figure 13). We also observed increased HSP27 protein expression (red fluorescence) detected with immunocytochemistry in EGFP-huA$_1$AR lentivirus-injected mice kidney (Figure 14). Furthermore, we saw increased colocalization (yellow) of HSP27 (red fluorescence) and EGFP-A$_1$AR (green fluorescence) in EGFP-huA$_1$AR lentivirus-injected mice kidney.

DISCUSSION

The major finding of this study is that overexpression of cytoprotective huA$_1$ARs in one kidney was sufficient to protect against liver and kidney injury after hepatic IR *in vivo*. We show that intraparenchymal injection of lentivirus preferentially expresses the transgene in the renal cortex and in the corticomedullary junction of the injected kidney. In mice renally injected with EGFP-huA$_1$AR lentivirus, there were significant protections against renal apoptosis, reduced renal tubular necrosis, inflammation, apoptosis, F-actin degradation, and better preservation of the integrity of the vascular endothelium. Plasma and tissue (injected kidney and liver) levels of cytokines (TNF-α and MCP-1) and ICAM-1 were significantly lower in mice renally injected with EGFP-huA$_1$AR lentivirus. Moreover mice injected with EGFP-huA$_1$AR showed reduced liver necrosis, inflammation, apoptosis, and F-actin degradation after liver IR. Removing the lentivirus-injected kidney before hepatic ischemia abolished the protective effects of renal EGFP-huA$_1$AR overexpression. Finally, we propose that the mechanism of improved renal and hepatic function after liver IR injury with intraparenchymal injection of EGFP-huA$_1$AR lentivirus is through induction of HSP27. Therefore, intrarenal lentiviral delivery of A$_1$ARs may potentially be used to protect against hepatic IR-induced kidney and liver injury.

Our previous studies showed that endogenous and exogenous A$_1$AR activation produced renal protection *in vivo* and *in vitro*.[8,9,14,26] Moreover, we recently showed that intrarenal injection of lentivirus encoding huA$_1$AR not only produced robust receptor expression in the injected kidney but this selective renal expression of huA$_1$ARs attenuated renal IR injury in mice lacking A$_1$ARs.[13] We concluded from

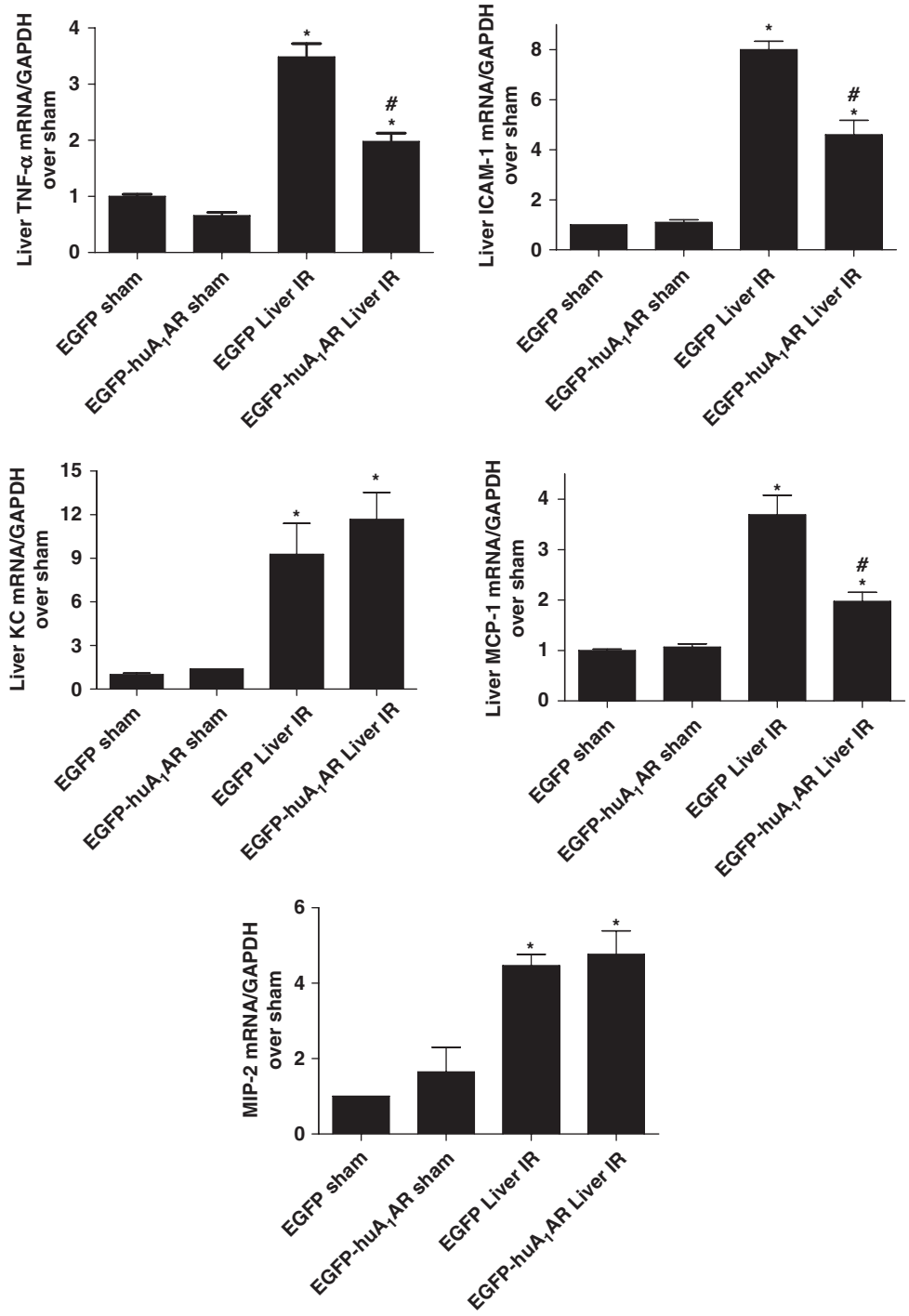

Figure 7 RT–PCR results for GAPDH, TNF-α, ICAM-1, KC, MCP-1, and MIP-2 mRNAs of liver tissue. Densitometric quantification of relative band intensities normalized to GAPDH from RT–PCR reactions was performed for each primer. C57BL/6 mice were subjected to sham-operation (sham) or liver IR 48 h after intrarenal injection with EGFP lentivirus or EGFP-huA$_1$AR lentivirus. The liver tissues were obtained 5 h after reperfusion. Data are presented as means ± s.e.m. $^*P<0.05$ *vs* sham group. $^\#P<0.05$ *vs* IR group.

these previous studies that upregulation of huA$_1$ARs in kidney is sufficient to produce increased cytoprotective signaling through activation of A$_1$ARs with endogenously produced mouse adenosine. Taking these concepts further, the most significant finding of this study is that selective overexpression of huA$_1$AR in one kidney was able to confer significant protection against both liver and kidney injury after hepatic IR in mice.

In this study, we show that renal injection of EGFP-huA$_1$AR encoding lentivirus significantly reduced proximal

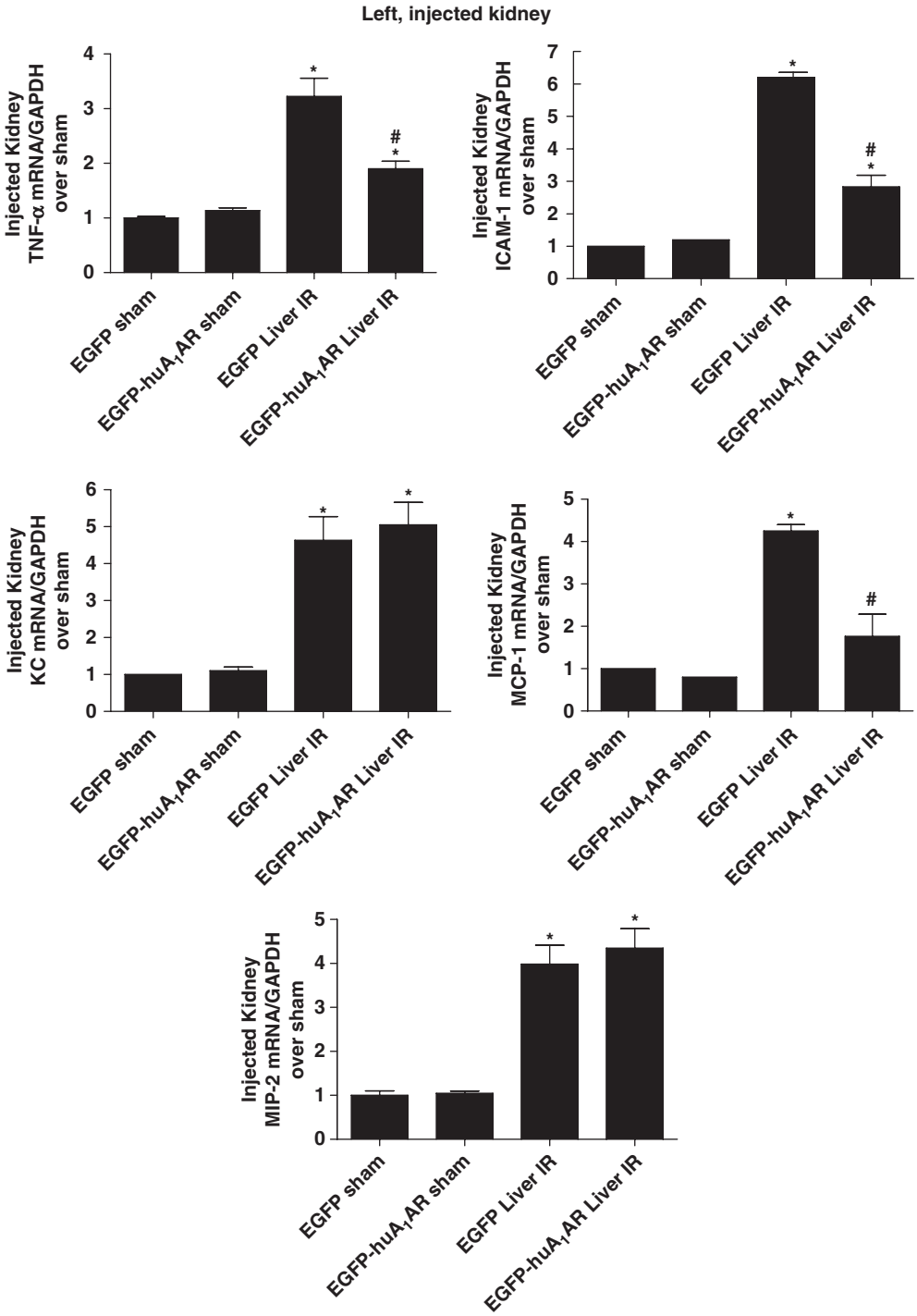

Figure 8 RT–PCR results for GAPDH, TNF-α, ICAM-1, KC, MCP-1, and MIP-2 mRNAs of kidney injected with lentivirus. Densitometric quantification of relative band intensities normalized to GAPDH from RT–PCR reactions was performed for each primer. C57BL/6 mice were subjected to sham-operation (sham) or liver IR 48 h after intrarenal injection with EGFP lentivirus or EGFP-huA$_1$AR lentivirus. The kidneys were obtained 5 h after reperfusion. Data are presented as means ± s.e.m. $^*P<0.05$ *vs* sham group. $^{\#}P<0.05$ *vs* IR group.

Figure 9 Representative fluorescent photomicrographs (TUNEL fluorescent stain) of liver (magnification × 100) and injected kidney (magnification × 100) sections illustrate apoptotic nuclei. C57BL/6 mice were subjected to sham-operation (sham) or liver IR 48 h after intrarenal injection with EGFP lentivirus or EGFP-huA$_1$AR lentivirus. Liver (**a**) and kidney (**b**) sections were obtained 24 h after reperfusion. Photographs are representative of six independent experiments. In kidney, endothelial cells not proximal tubule cells underwent apoptosis.

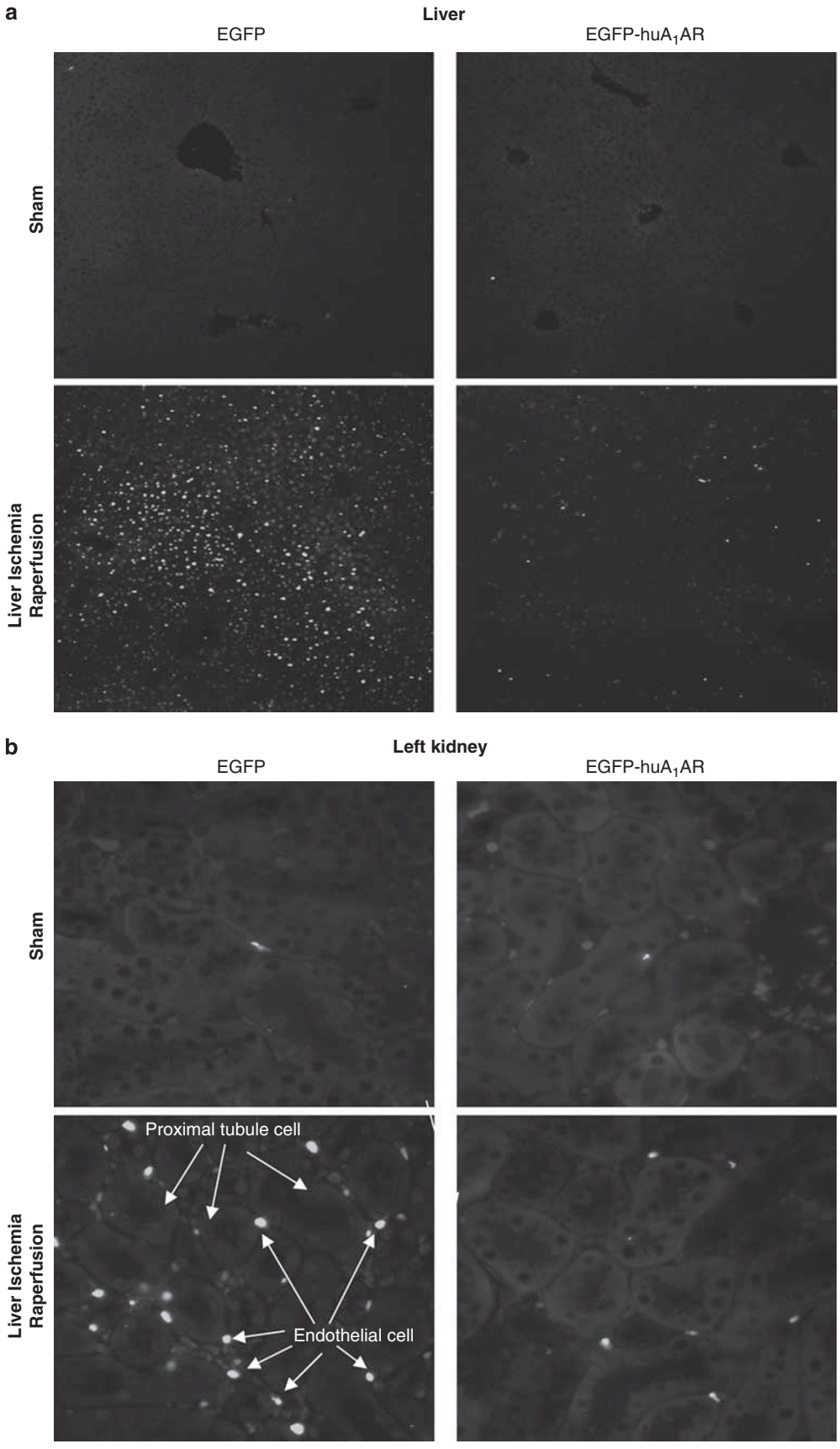
a
Liver
EGFP
EGFP-huA1AR
Sham
Liver Ischemia Raperfusion
b
Left kidney
EGFP
EGFP-huA1AR
Sham
Liver Ischemia Raperfusion
Proximal tubule cell
Endothelial cell

tubule necrosis, vacuolization and simplification, and decreased the necrosis of liver parenchyma after liver IR. Furthermore, we show that overexpression of huA_1AR in one kidney was able to suppress apoptotic cell death of the liver and the injected kidney after liver IR (reduced TUNEL staining, DNA laddering and caspase 3 fragmentation). Therefore, direct protection against renal injury with intrarenal injection of lentivirus encoding EGFP-huA_1AR also protected against hepatic injury after liver IR. Necrotic liver cell death occurs directly by total breakdown of cellular homeostatic machinery secondary to massive depletion of ATP during and after the ischemic period. Necrosis also occurs during reperfusion where uncontrolled delivery of cytotoxic cytokines and/or free radicals cause further cellular derangements.[27] We believe the major changes in renal histology occur after reperfusion of the ischemic liver. The clinical significance of our finding is that the impairment in renal function after liver IR potentiates liver dysfunction *in vivo* and protecting the kidney can lead to liver protection after hepatic IR. The kidney, therefore, has an important role in modulating hepatic injury and necrosis after liver IR.

We achieved selective transduction of both EGFP and EGFP-huA_1AR in the lentivirus-injected kidneys indicated by a lack of green fluorescence in the contralateral kidneys, heart, or lungs of mice renally injected with lentivirus. RT–PCR also showed that the injected transgene was concentrated within the cortices-injected kidney (Figure 1b). We further confirmed the selective protein expression resulting from lentivirus injections by demonstrating that mice renally injected with EGFP-huA_1AR lentivirus express huA_1AR protein (immunocytochemistry; Figure 2) whereas mice injected with EGFP lentivirus do not. Therefore, our method of lentiviral gene delivery allowed us to directly test the hypothesis that overexpression of huA_1AR expression in kidneys of mice through intrarenal injection improves renal function after liver IR injury. The expression of transgene (EGFP or EGFP-huA_1AR) was observed primarily in the cortex and at the corticomedullary junction. At this site, there are primarily S3 segments of proximal tubule as the major tubular segment represented. Expression was nearly undetectable in the inner medulla where there is a concentration of collecting ducts and thin limbs of Henle. The major site of endothelial cell injury in our model of liver IR predominantly affects the 'outer stripe' of the outer medulla corresponding to the S3 segments of proximal tubule, which is located precisely at the corticomedullary junction.[28,29]

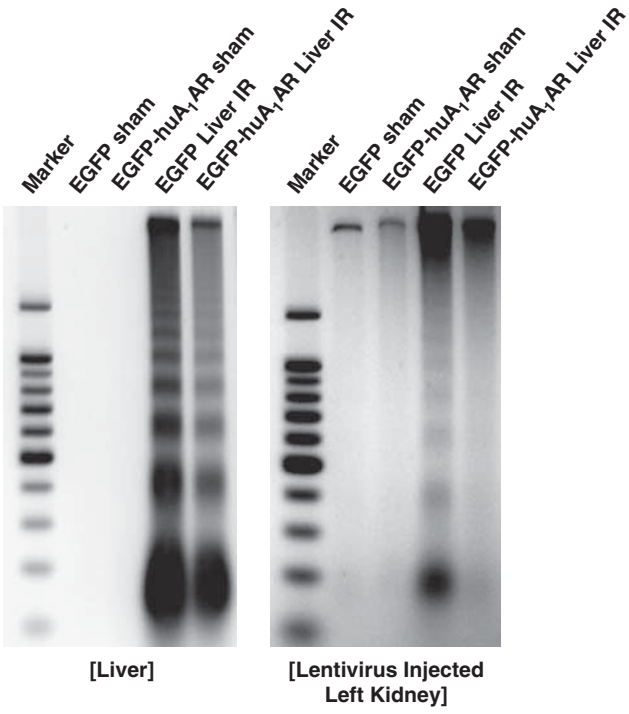

Figure 10 Representative gel images showing DNA laddering as an index of DNA fragmentations in liver and kidney tissues. C57BL/6 mice were subjected to sham-operation (sham) or liver IR 48 h after intrarenal injection with EGFP lentivirus or EGFP-huA_1AR lentivirus. Liver and kidney tissues were obtained 24 h after reperfusion. Representative of five independent experiments.

The production of several proinflammatory cytokines and adhesion molecules after hepatic IR contributes to the pathophysiology of liver injury.[1,30] We show that as expected, all of the proinflammatory mRNAs examined (TNF-α KC, MCP-1, MIP-2, and ICAM-1) show enhanced expression in liver and kidney after hepatic IR. We also show that plasma and tissue (injected kidney and liver) levels of cytokines (TNF-α and MCP-1) and ICAM-1 were significantly lower in mice renally injected with EGFP-huA_1AR lentivirus. TNF-α is a well known mediator of liver and kidney injury after IR.[31,32] TNF-α is known to promote the migration of inflammatory cells into the renal parenchyma through the upregulation of MCP-1 and MIP-2 in kidney.[33] The CC chemokine MCP-1 and CXC chemokine MIP-2 are also important mediators in the pathogenesis of AKI.[34] Upregulation of MCP-1 and MIP-2 leads to neutrophil recruitment during AKI induced by renal IR or nephrotoxic agents.[35] Indeed, our study showed that liver IR not only caused rapid infiltration of neutrophils into liver but also caused neutrophil infiltration in kidney. The role of neutrophils in the pathophysiology of organ injury (including liver and kidney) is well recognized.[36] Overexpression of huA_1AR in kidney was able to suppress several proinflammatory mRNAs (TNF-α, MCP-1, and ICAM-1) in liver and kidney. Furthermore, overexpression of huA_1AR in kidney was able to suppress PMN infiltration in both liver and kidney with concomitant improvements in vascular endothelial cell integrity (indicated by reduced EBD infiltration).

Ischemia–reperfusion injury *in vivo* results in F-actin cytoskeleton degradation which further compromises organ function.[37,38] For example, F-actin disruption is a well known stimulus of apoptosis in several cell lines.[39] We saw severe disruption of F-actin in liver and kidney proximal tubules after liver IR in EGFP lentivirus-injected mice. Specifically,

we saw severe disruptions in both hepatocyte and bile canalicular F-actin cytoskeleton after liver IR (Figure 11). Moreover, proximal tubule brush border F-actin was completely disrupted after liver IR (Figure 11). We showed in this study that huA_1AR overexpression in kidney resulted in markedly better preserved F-actin of liver and kidney. Intact F-actin cytoskeleton in liver and kidney of mice subjected to liver IR may have contributed to reduced necrosis and apoptosis observed in these mice.

We showed in this study that intrarenal injection of EGFP-huA_1AR lentivirus increased HSP27 mRNA and protein in the injected kidney only without increasing the HSP27 expression in the contralateral kidney or in the liver. We previously showed that A_1AR activation led to the synthesis of new HSP27 *in vitro*[14] and *in vivo*.[40] Therefore, overexpression of EGFP-huA_1AR in mice may produce renal protection through the induction of HSP27 in the injected kidneys. HSP27 is a member of family of chaperone proteins that are upregulated in response to a wide range of cellular stresses including hypoxia, ischemia, and exposure to toxic drugs.[41–44] Increased expression of HSP27 serves to defend a cell against injury or death by acting as chaperones facilitating proper polypeptide folding and aberrant protein removal.[45–47] Furthermore, HSP27 is a potent anti-apoptotic protein and is a key stabilizer of the actin cytoskeleton; both of these cellular effects lead to increased resistance against cell death.[48–50] We previously showed that intrarenal injection of EGFP-huA_1AR lentivirus in mice not only increased the HSP27 expression but also increased colocalization of HSP27 with F-actin *in vivo*.[13] Indeed, stress or injury in renal tubule cells promote association or colocalization of HSP27 with F-actin leading to cytoprotection *in vitro*.[51,52] We propose that renal overexpression of huA_1ARs led to increased HSP27 synthesis in the injected kidney with resultant F-actin stabilization with subsequent protection against AKI after liver IR.

We also show in this study that renal huA_1AR overexpression is directly responsible for both hepatic and renal protection after liver IR in mice as removing the EGFP-huA_1AR overexpressing kidney before liver IR completely abolished the hepatic and renal protective effects observed in these mice. Removing the lentivirus-injected kidney before

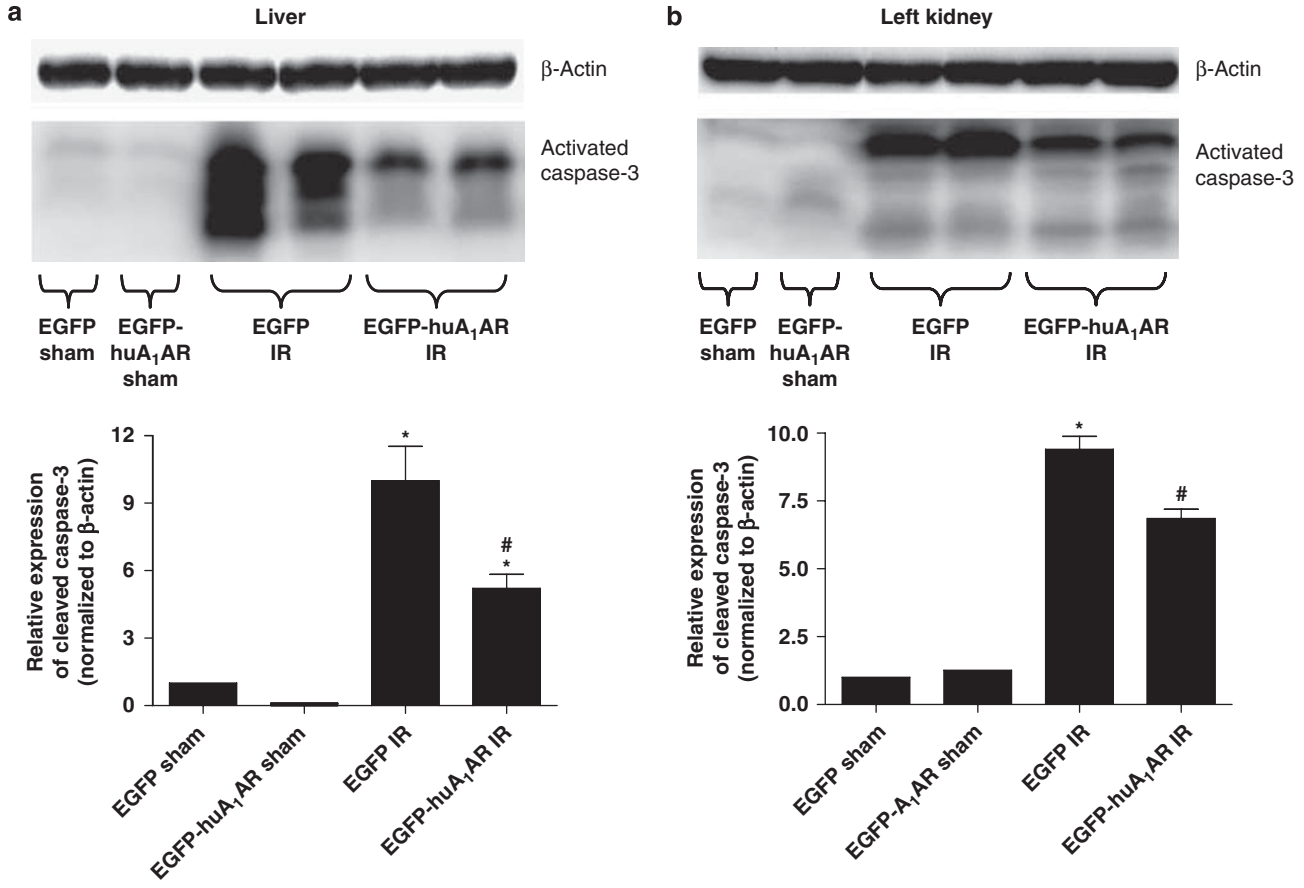

Figure 11 Top: representative β-actin and caspase 3 fragmentation immunoblotting in liver (**a**) and kidney (**b**) tissues. C57BL/6 mice were subjected to sham-operation (sham) or liver IR 48 h after intrarenal injection with EGFP lentivirus or EGFP-huA_1AR lentivirus. Liver and kidney tissues were obtained 24 h after reperfusion. Photographs are representative of four independent experiments. Bottom: densitometric quantifications of cleaved caspase 3 (normalized to β-actin) in mice subjected to sham-operation or liver IR ($N=4$ for each group). $^{*}P<0.05$ *vs* sham group. $^{\#}P<0.05$ *vs* IR group.

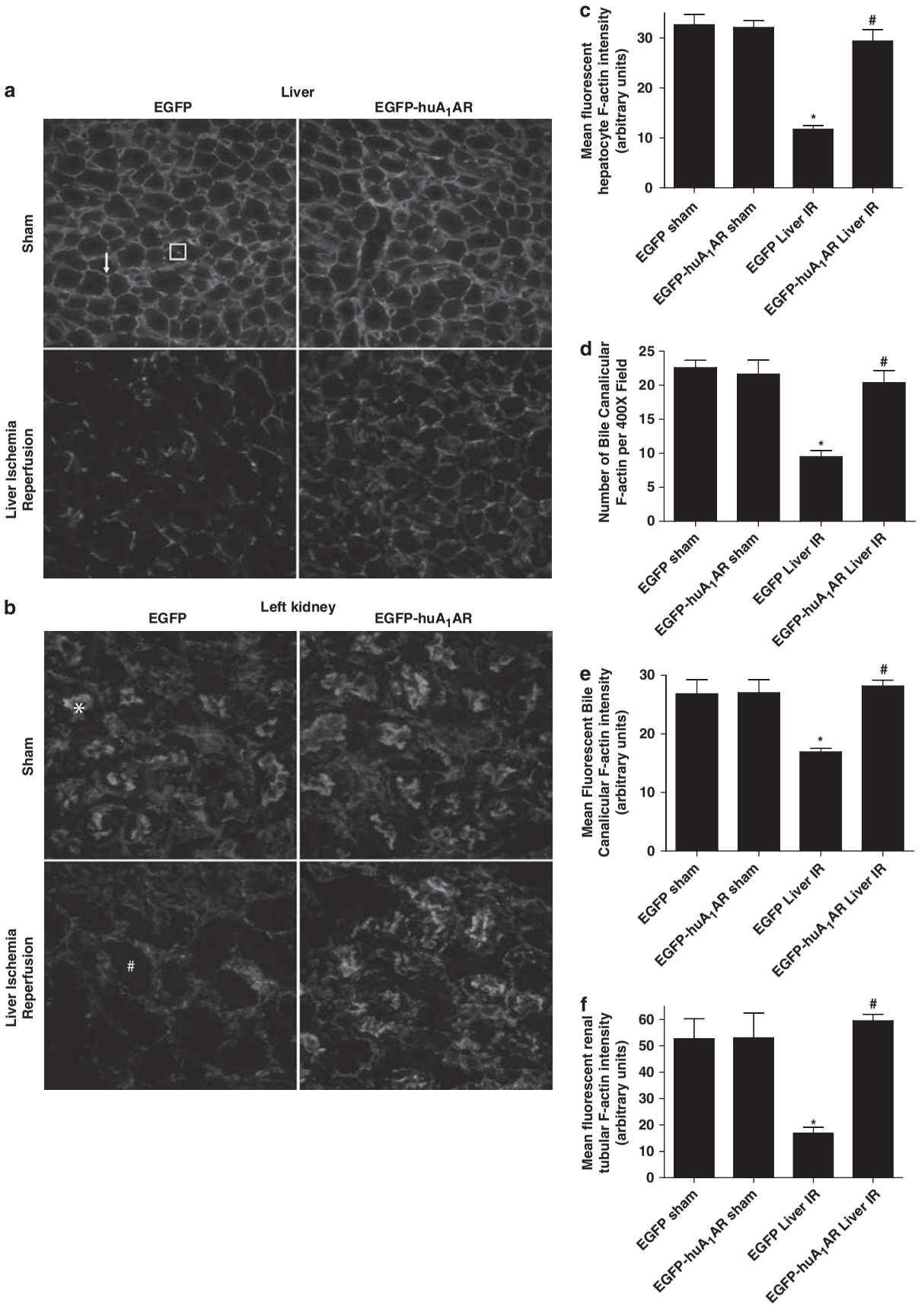
a
Liver
EGFP
EGFP-huA1AR
Sham
Liver Ischemia Reperfusion
b
Left kidney
EGFP
EGFP-huA1AR
Sham
Liver Ischemia Reperfusion
c
Mean fluorescent hepatocyte F-actin intensity (arbitrary units)
EGFP sham
EGFP-huA1AR sham
EGFP Liver IR
EGFP-huA1AR Liver IR
d
Number of Bile Canalicular F-actin per 400X Field
e
Mean Fluorescent Bile Canalicular F-actin intensity (arbitrary units)
f
Mean fluorescent renal tubular F-actin intensity (arbitrary units)

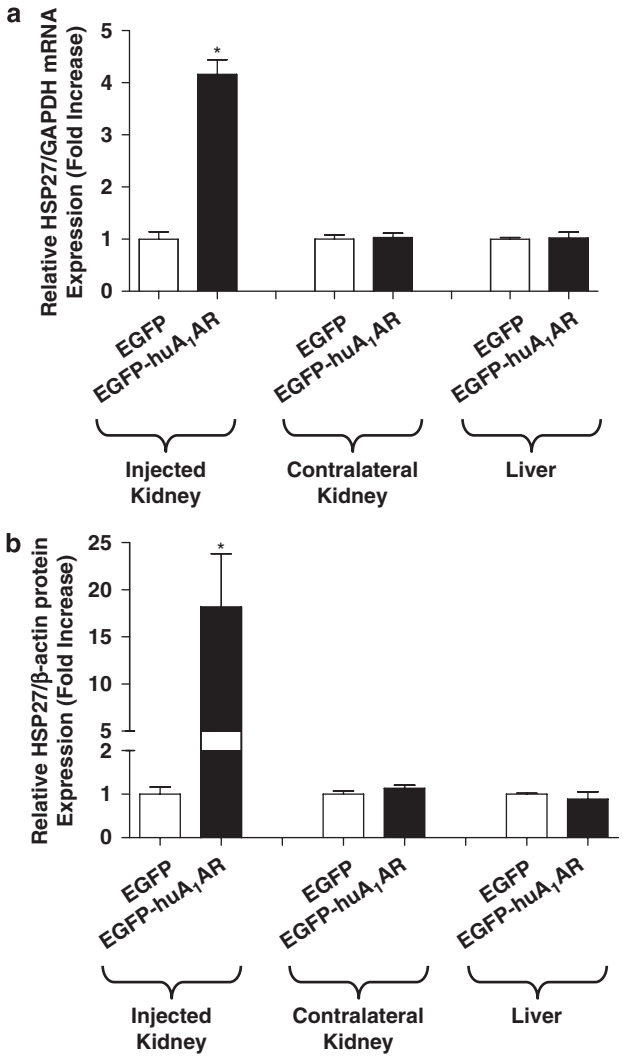

Figure 13 (**a**) Densitometric quantifications of relative band intensities from RT–PCR reactions ($N=4$) for HSP27 mRNA (normalized to GAPDH) processed from lentivirus (EGFP or EGFP-huA$_1$AR) injected kidney, from contralateral (non-lentivirus-injected) kidney or from liver. C57 mice kidneys were renally injected with EGFP encoding lentivirus or EGFP-huA$_1$AR encoding lentivirus 48 h before RT–PCR. Data in bar graphs are means ± s.e.m. $^*P<0.05$ *vs* EGFP lentivirus-injected tissue. (**b**) Densitometric quantifications of relative band intensities from immunoblotting for murine HSP27 ($N=4$, normalized to β-actin protein). Data in bar graphs are means ± s.e.m. $^{\#}P<0.05$ *vs* EGFP injected mice.

liver IR increased the plasma cytokine and ICAM-1 levels (Table 2). Furthermore, removing the lentivirus-injected kidney before liver IR also abolished the reductions in plasma levels of cytokines and ICAM-1 in mice renally injected with EGFP-huA$_1$AR lentivirus (Table 2). Taken together, data from these cohorts of mice also confirm that systemic spill over of EGFP-huA$_1$AR lentivirus (to contralateral kindey and/or to liver) cannot explain the hepatic and renal protective effects with EGFP-huA$_1$AR lentivirus injection. Instead, we propose that direct EGFP-huA$_1$AR-mediated reduction in AKI through HSP27 induction produced direct hepatic protection after IR. Our findings imply that liver IR-mediated AKI potentiates the liver injury further and protecting the kidney function causes reduction of liver damage after IR.

One of the limitations of the intraparenchymal injection of virus is that we cannot control the expression of the protective transgene in a specific cell type (eg, proximal tubule cells of the S3 segment). However, we show in this study that intraparenchymal injection of lentivirus encoding EGFP-huA$_1$AR led to heavy expression in the cortex and proximal tubules. These are the areas that are the most susceptible to injury because of the precarious balance between oxygen supply and demand, high ATP consumption, and relatively low blood flow.

In summary, we show in this study that selective expression of huA$_1$AR transgene in kidney is possible. We not only show renal protection but also observed improved liver function after intrarenal injection with huA$_1$AR lentivirus in mice subjected to liver IR. Overexpression of huA$_1$AR in the injected kidney was able to improve vascular integrity and reduce necrosis, apoptosis, and inflammation in both liver and kidney. We propose that huA$_1$AR-mediated induction of HSP27 results in increased resistance against renal injury after liver IR leading to reduced liver injury as a consequence. HSP27 induction after huA$_1$AR overexpression may reduce the necrotic, apoptotic, and inflammatory changes occurring in the injected kidney and liver providing overall renal and hepatic protection against liver IR. These findings may have important clinical implications as they imply that kidney-specific expression of A$_1$ARs through lentiviral delivery is a viable therapeutic option in attenuating the effects of hepatic IR.

Figure 12 (**a** and **b**) Representative fluorescent photomicrographs of phalloidin staining of the liver and kidney tissues (magnification × 400). C57BL/6 mice were subjected to sham-operation (sham) or liver IR 48 h after intrarenal injection with EGFP lentivirus or EGFP-huA$_1$AR lentivirus. Liver (**a**) and kidney (**b**) tissues were obtained 24 h after reperfusion. In liver, F-actin is localized in basolateral membranes (arrow) and bile canalicular membranes. Transverse sections of bile canaliculi are seen as typical dots (square). After liver IR in EGFP lentivirus mice, the basolateral and bile canalicular membrane F-actin stains were reduced and disorganized. In kidney, F-actin stains of proximal tubular epithelial cells are prominent in the brush border from sham-operated mice (*) that is severely degraded in kidneys of mice subjected to liver IR after EGFP lentivirus injection (#). Photographs are representative of five independent experiments. (**c**-**f**) Quantification of mean fluorescent hepatocyte F-actin intensity (**c**, $N=5$), number of intact bile canalicular membranes (**d**, $N=5$) and mean fluorescent intensities of bile canalicular membranes (**e**, $N=5$) and renal proximal tubule (**f**, $N=5$) F-actin intensity as measures of F-actin preservation in liver and kidney sections. $^*P<0.05$ *vs* sham group. $^{\#}P<0.05$ *vs* IR group.

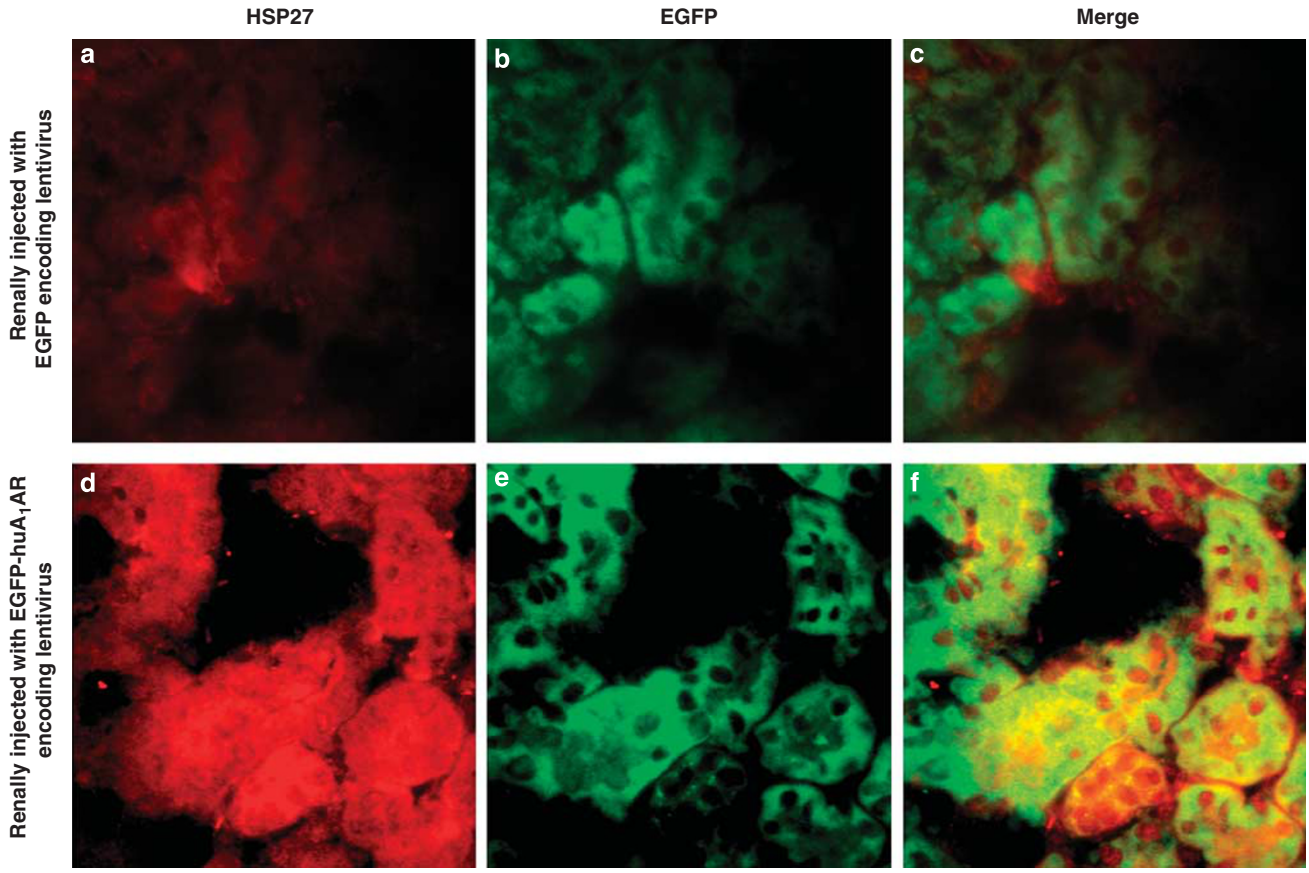

Figure 14 Representative fluorescent photomicrographs of kidney HSP27 (red, **a**, **d**) and EGFP expression (green, **b**, **e**) in mice renally injected with either EGFP (**a**,**b**,**c**) or EGFP-huA$_1$AR lentivirus (**d**,**e**,**f**) before 48 h. With 0.25 μm thick *Z*-sections, we were able to show that murine HSP27 (red, **a**, **d**) and EGFP-huA$_1$ARs (green, **b**, **e**) colocalize together (yellow, **e**, **f**). Representative of five independent experiments.

Supplementary Information accompanies the paper on the Laboratory Investigation website (http://www.laboratoryinvestigation.org)

ACKNOWLEDGEMENT

This work was supported by the National Institute of Health Grant RO1 DK-58547.

DISCLOSURE/CONFLICT OF INTEREST

The authors declare no conflict of interest.

1. Serracino-Inglott F, Habib NA, Mathie RT. Hepatic ischemia–reperfusion injury. Am J Surg 2001;181:160–166.
2. Fondevila C, Busuttil RW, Kupiec-Weglinski JW. Hepatic ischemia/reperfusion injury—a fresh look. Exp Mol Pathol 2003;74:86–93.
3. Behrends M, Hirose R, Park YH, *et al.* Remote renal injury following partial hepatic ischemia/reperfusion injury in rats. J Gastrointest Surg 2008;12:490–495.
4. Weinbroum AA, Hochhauser E, Rudick V, *et al.* Direct induction of acute lung and myocardial dysfunction by liver ischemia and reperfusion. J Trauma 1997;43:627–633.
5. Davis CL, Gonwa TA, Wilkinson AH. Pathophysiology of renal disease associated with liver disorders: implications for liver transplantation. Part I. Liver Transpl 2002;8:91–109.
6. Kielar ML, John R, Bennett M, *et al.* Maladaptive role of IL-6 in ischemic acute renal failure. J Am Soc Nephrol 2005;16:3315–3325.
7. Lee HT, Park SW, Kim M, *et al.* Acute kidney injury after hepatic ischemia and reperfusion injury in mice. Lab Invest 2009;89:196–208.
8. Lee HT, Gallos G, Nasr SH, *et al.* A1 adenosine receptor activation inhibits inflammation, necrosis, and apoptosis after renal ischemia–reperfusion injury in mice. J Am Soc Nephrol 2004;15:102–111.
9. Lee HT, Xu H, Nasr SH, *et al.* A1 adenosine receptor knockout mice exhibit increased renal injury following ischemia and reperfusion. Am J Physiol Renal Physiol 2004;286:F298–F306.
10. Lee HT, Emala CW. Protein kinase C and G(i/o) proteins are involved in adenosine- and ischemic preconditioning-mediated renal protection. J Am Soc Nephrol 2001;12:233–240.
11. Lee HT, Emala CW. Protective effects of renal ischemic preconditioning and adenosine pretreatment: role of A(1) and A(3) receptors. Am J Physiol Renal Physiol 2000;278:F380–F387.
12. Kim J, Kim M, Song JH, *et al.* Endogenous A1 adenosine receptors protect against hepatic ischemia reperfusion injury in mice. Liver Transpl 2008;14:845–854.
13. Kim M, Chen SW, Park SW, *et al.* Kidney-specific reconstitution of the A1 adenosine receptor in A1 adenosine receptor knockout mice reduces renal ischemia–reperfusion injury. Kidney Int 2009;75:809–823.
14. Lee HT, Kim M, Jan M, *et al.* Renal tubule necrosis and apoptosis modulation by A1 adenosine receptor expression. Kidney Int 2007;71(12):1249–1261.
15. Lee HT, Jan M, Bae SC, *et al.* A1 adenosine receptor knockout mice are protected against acute radiocontrast nephropathy *in vivo*. Am J Physiol Renal Physiol 2006;290:F1367–F1375.
16. Nakamura A, Imaizumi A, Yanagawa Y, *et al.* beta(2)-Adrenoceptor activation attenuates endotoxin-induced acute renal failure. J Am Soc Nephrol 2004;15:316–325.
17. Lee HT, Emala CW, Joo JD, *et al.* Isoflurane improves survival and protects against renal and hepatic injury in murine septic peritonitis. Shock 2007;27:373–379.

18. Lee HT, Kim M, Kim J, *et al.* TGF-beta1 release by volatile anesthetics mediates protection against renal proximal tubule cell necrosis. Am J Nephrol 2007;27:416–424.
19. SLOT C. Plasma creatinine determination. A new and specific Jaffe reaction method. Scand J Clin Lab Invest 1965;17: 381–387.
20. Suzuki S, Toledo-Pereyra LH, Rodriguez FJ, *et al.* Neutrophil infiltration as an important factor in liver ischemia and reperfusion injury. Modulating effects of FK506 and cyclosporine. Transplantation 1993;55:1265–1272.
21. Awad AS, Ye H, Huang L, *et al.* Selective sphingosine 1–phosphate 1 receptor activation reduces ischemia–reperfusion injury in mouse kidney. Am J Physiol Renal Physiol 2006;290:F1516–F1524.
22. Chen SW, Park SW, Kim M, *et al.* Human heat shock protein 27 overexpressing mice are protected against hepatic ischemia and reperfusion injury. Transplantation 2009;87:1478–1487.
23. Herrmann M, Lorenz HM, Voll R, *et al.* A rapid and simple method for the isolation of apoptotic DNA fragments. Nucleic Acids Res 1994;22:5506–5507.
24. Molitoris BA. Putting the actin cytoskeleton into perspective: pathophysiology of ischemic alterations. Am J Physiol 1997;272: F430–F433.
25. Suzuki S, Toledo-Pereyra LH, Rodriguez FJ, *et al.* Neutrophil infiltration as an important factor in liver ischemia and reperfusion injury. Modulating effects of FK506 and cyclosporine. Transplantation 1993;55:1265–1272.
26. Lee HT, Emala CW. Preconditioning and adenosine protect human proximal tubule cells in an *in vitro* model of ischemic injury. J Am Soc Nephrol 2002;13:2753–2761.
27. Saikumar P, Dong Z, Weinberg JM, *et al.* Mechanisms of cell death in hypoxia/reoxygenation injury. Oncogene 1998;17:3341–3349.
28. Epstein FH, Brezis M, Silva P, *et al.* Physiological and clinical implications of medullary hypoxia. Artif Organs 1987;11:463–467.
29. Heyman SN, Brezis M, Reubinoff CA, *et al.* Acute renal failure with selective medullary injury in the rat. J Clin Invest 1988;82: 401–412.
30. Frangogiannis NG. Chemokines in ischemia and reperfusion. Thromb Haemost 2007;97:738–747.
31. Donnahoo KK, Meldrum DR, Shenkar R, *et al.* Early renal ischemia, with or without reperfusion, activates NFkappaB and increases TNF-alpha bioactivity in the kidney. J Urol 2000;163:1328–1332.
32. Meldrum DR, Donnahoo KK. Role of TNF in mediating renal insufficiency following cardiac surgery: evidence of a postbypass cardiorenal syndrome. J Surg Res 1999;85:185–199.
33. Ramesh G, Reeves WB. TNF-alpha mediates chemokine and cytokine expression and renal injury in cisplatin nephrotoxicity. J Clin Invest 2002;110:835–842.
34. Furuichi K, Wada T, Iwata Y, *et al.* CCR2 signaling contributes to ischemia–reperfusion injury in kidney. J Am Soc Nephrol 2003;14:2503–2515.
35. Miura M, Fu X, Zhang QW, *et al.* Neutralization of Gro alpha and macrophage inflammatory protein-2 attenuates renal ischemia/ reperfusion injury. Am J Pathol 2001;159:2137–2145.
36. Jaeschke H. Mechanisms of liver injury. II. Mechanisms of neutrophil-induced liver cell injury during hepatic ischemia–reperfusion and other acute inflammatory conditions. Am J Physiol Gastrointest Liver Physiol 2006;290:G1083–G1088.
37. Benkoel L, Dodero F, Hardwigsen J, *et al.* Effect of ischemia–reperfusion on bile canalicular F-actin microfilaments in hepatocytes of human liver allograft: image analysis by confocal laser scanning microscopy. Dig Dis Sci 2001;46:1663–1667.
38. Kellerman PS, Norenberg SL, Jones GM. Early recovery of the actin cytoskeleton during renal ischemic injury *in vivo*. Am J Kidney Dis 1996;27:709–714.
39. White SR, Williams P, Wojcik KR, *et al.* Initiation of apoptosis by actin cytoskeletal derangement in human airway epithelial cells. Am J Respir Cell Mol Biol 2001;24:282–294.
40. Joo JD, Kim M, Horst P, *et al.* Acute and delayed renal protection against renal ischemia and reperfusion injury with A1 adenosine receptors. Am J Physiol Renal Physiol 2007;293:F1847–F1857.
41. Garrido C, Bruey JM, Fromentin A, *et al.* HSP27 inhibits cytochrome c-dependent activation of procaspase-9. FASEB J 1999;13:2061–2070.
42. Bruey JM, Ducasse C, Bonniaud P, *et al.* Hsp27 negatively regulates cell death by interacting with cytochrome c. Nat Cell Biol 2000;2:645–652.
43. Arrigo AP, Firdaus WJ, Mellier G, *et al.* Cytotoxic effects induced by oxidative stress in cultured mammalian cells and protection provided by Hsp27 expression. Methods 2005;35:126–138.
44. Arrigo AP. Hsp27: novel regulator of intracellular redox state. IUBMB Life 2001;52:303–307.
45. Wyttenbach A, Sauvageot O, Carmichael J, *et al.* Heat shock protein 27 prevents cellular polyglutamine toxicity and suppresses the increase of reactive oxygen species caused by huntingtin. Hum Mol Genet 2002;11:1137–1151.
46. Samali A, Robertson JD, Peterson E, *et al.* Hsp27 protects mitochondria of thermotolerant cells against apoptotic stimuli. Cell Stress Chaperones 2001;6:49–58.
47. Paul C, Manero F, Gonin S, *et al.* Hsp27 as a negative regulator of cytochrome C release. Mol Cell Biol 2002;22:816–834.
48. Weber NC, Toma O, Wolter JI, *et al.* Mechanisms of xenon- and isoflurane-induced preconditioning—a potential link to the cytoskeleton via the MAPKAPK-2/HSP27 pathway. Br J Pharmacol 2005;146:445–455.
49. Landry J, Huot J. Regulation of actin dynamics by stress-activated protein kinase 2 (SAPK2)-dependent phosphorylation of heat-shock protein of 27 kDa (Hsp27). Biochem Soc Symp 1999;64:79–89.
50. Huot J, Houle F, Spitz DR, *et al.* HSP27 phosphorylation-mediated resistance against actin fragmentation and cell death induced by oxidative stress. Cancer Res 1996;56:273–279.
51. Van Why SK, Mann AS, Ardito T, *et al.* Hsp27 associates with actin and limits injury in energy depleted renal epithelia. J Am Soc Nephrol 2003;14:98–106.
52. Shelden EA, Borrelli MJ, Pollock FM, *et al.* Heat shock protein 27 associates with basolateral cell boundaries in heat-shocked and ATP-depleted epithelial cells. J Am Soc Nephrol 2002;13: 332–341.